




## ForceSticker: Wireless, Batteryless, Thin & Flexible Force Sensors


AGRIM GUPTA , Electrical & Computer Engineering, UC San Diego, USA


DAEGUE PARK , Mechanical & Aerospace Engineering, UC San Diego, USA

SHAYAUN BASHAR , Electrical & Computer Engineering, UC San Diego, USA

CEDRIC GIRERD , Mechanical & Aerospace Engineering, UC San Diego, USA

NAGARJUN BHAT , Electrical & Computer Engineering, UC San Diego, USA

SIDDHI MUNDHRA , Foothill High School, Pleasanton, USA

TANIA K. MORIMOTO , Mechanical & Aerospace Engineering, UC San Diego, USA







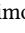

DINESH BHARADIA , Electrical & Computer Engineering, UC San Diego, USA

Any two objects in contact with each other exert a force that could be simply due to gravity or mechanical contact, such as any ubiquitous object exerting weight on a platform or the contact between two bones at our knee joints. The most ideal way of capturing these contact forces is to have a flexible force sensor which can conform well to the contact surface. Further, the sensor should be thin enough to not affect the contact physics between the two objects. In this paper, we showcase the design of such thin, flexible sticker-like force sensors dubbed as ‘ForceStickers’, ushering into a new era of miniaturized force sensors. ForceSticker achieves this miniaturization by creating new class of capacitive force sensors which avoid both batteries, as well as wires. The wireless and batteryless readout is enabled via hybrid analog-digital backscatter, by piggybacking analog sensor data onto a digitally identified RFID link. Hence, ForceSticker finds natural applications in space and battery-constraint in-vivo usecases, like force-sensor backed orthopaedic implants, surgical robots. Further, ForceSticker finds applications in ubiquiti-constraint scenarios. For example, these force-stickers enable cheap, digitally readable barcodes that can provide weight information, with possible usecases in warehouse integrity checks. To meet these varied application scenarios, we showcase the general framework behind design of ForceSticker. With ForceSticker framework, we design 4mm\*2mm sensor prototypes, with two different polymer layers of ecoflex and neoprene rubber, having force ranges of 0-6N and 0-40N respectively, with readout errors of 0.25, 1.6 N error each (<5% of max. force). Further, we stress test ForceSticker by >10,000 force applications without significant error degradation. We also showcase two case-studies onto the possible applications of ForceSticker: sensing forces from a toy knee-joint model and integrity checks of warehouse packaging.

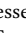

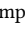

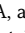
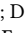
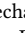

CCS Concepts: • **Hardware** → **Wireless devices; Sensor applications and deployments; Sensor devices and platforms.**

Additional Key Words and Phrases: Force sensors, Capacitive Sensors, RFID systems, Hybrid Backscatter, Haptic Interfaces, Batteryless Sensors, Small Antennas, Phase Sensing, Multiphysics Simulations

### ACM Reference Format:

Agrim Gupta , Daegue Park , Shayaun Bashar , Cedric Girerd , Nagarjun Bhat , Siddhi Mundhra , Tania K. Morimoto , and Dinesh Bharadia . 2023. ForceSticker: Wireless, Batteryless, Thin & Flexible Force Sensors. *Proc. ACM Interact. Mob. Wearable Ubiquitous Technol.* 7, 1, Article 13 (March 2023), 32 pages. <https://doi.org/10.1145/3580793>

This research was supported in part by the National Science Foundation under Grant 1935329.

Authors' addresses: Agrim Gupta , Electrical & Computer Engineering, UC San Diego, USA, [agg003@ucsd.edu](mailto:agg003@ucsd.edu); Daegue Park , Mechanical & Aerospace Engineering, UC San Diego, USA, [d8park@ucsd.edu](mailto:d8park@ucsd.edu); Shayaun Bashar , Electrical & Computer Engineering, UC San Diego, USA, [sbashar@ucsd.edu](mailto:sbashar@ucsd.edu); Cedric Girerd , Mechanical & Aerospace Engineering, UC San Diego, USA, [cgirerd@ucsd.edu](mailto:cgirerd@ucsd.edu); Nagarjun Bhat , Electrical & Computer Engineering, UC San Diego, USA, [nbhat@ucsd.edu](mailto:nbhat@ucsd.edu); Siddhi Mundhra , Foothill High School, Pleasanton, USA, [siddhimundhra201105@gmail.com](mailto:siddhimundhra201105@gmail.com); Tania K. Morimoto , Mechanical & Aerospace Engineering, UC San Diego, USA, [tkmorimoto@ucsd.edu](mailto:tkmorimoto@ucsd.edu); Dinesh Bharadia , Electrical & Computer Engineering, UC San Diego, USA, [dineshb@ucsd.edu](mailto:dineshb@ucsd.edu).



This work is licensed under a Creative Commons Attribution International 4.0 License.

© 2023 Copyright held by the owner/author(s).

2474-9567/2023/3-ART13

<https://doi.org/10.1145/3580793>

## 1 INTRODUCTION

Force is a ubiquitous phenomenon in our daily environment, with any two objects in contact exerting forces onto each other. This phenomenon can take many different forms, from the weight (gravitational force) of an object on a table to the grip force of a human hand or robotic manipulator, and even the impact forces experienced by our joints when bones come into contact. Hence, force-sensors are envisioned to have multiple applications as they record these different contact phenomenon, ranging from knee-joint implant health [1, 2] to robotic control [3–5] and even enabling new AR/VR interfaces [6–8]. To enable these various applications, it's crucial for the force-sensors to conform closely to the objects in contact, and this necessitates a thin and flexible design, akin to a sticker.

To better concretize the requirements of these thin and flexible sticker-like force sensors, consider the force-sensor backed orthopaedic implant application as shown in Figure 1e, with similar requirements required for other applications as well.

- **R1. Flexible and thin form-factor:** By sensing the impact forces at knee-joint, the health of the implant as well as the correctness of implant's fit can be determined [1, 2]. However, in order to fit snugly in the narrow and non-uniform contact surface between the implant and tissues/bones, the force sensors need to be thin and flexible.
- **R2. Wireless Readout:** Today, we have thin force sensitive resistors [9–11], capacitors [12–14], or piezos [15–17] available which by themselves may fit to the required form factors. These sensors are read by a readout-device (Fig. 2a), typically via a wired connection between the two devices. Further, additional electronics like amplifiers may be required near the sensors, to facilitate the sensor readings communication. The sensors, with extra interfacing electronics forms a combined 'sensor-device'. Now, for the in-vivo applications, it would be impractical to assume a wired connection from the 'sensor-device' present in the implant inside body to the 'reader-device' held by a user outside of body [18–20]. Hence, we need a mechanism to somehow support wireless readout of the sensor-device via the remotely located reader-device.
- **R3. Battery-free and Low-power:** A straightforward method of making wireless sensor-devices is by transmitting the analog sensor data via Wi-Fi/Bluetooth. This requires electronics to first digitize the analog sensor readings into bits using ADCs (Analog-to-Digital convertors) and then transmitting the bits across using Wi-Fi/Bluetooth RFICs (Radio Frequency Integrated Circuits). This can make the wireless

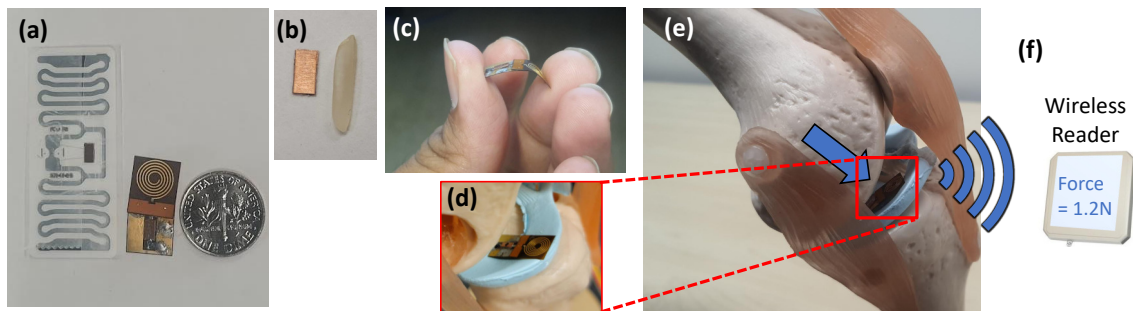


Fig. 1. (a) Shows 2 versions of ForceSticker, integrated with standard RFID stickers and a small flexible PCB (b) Shows the sensor by itself, compared to a rice grain (c) Demonstrates the flexibility of the sensor PCB designed (d,e,f) Shows how ForceSticker can be used for in-vivo implant force sensing read wirelessly via an remotely located reader

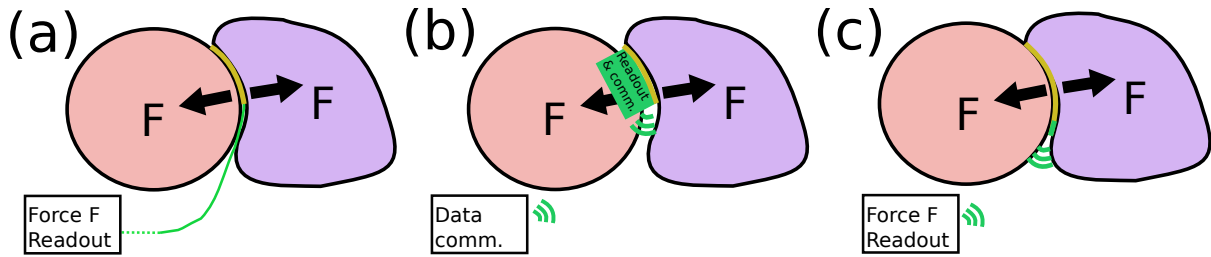


Fig. 2. (a) Shows miniaturized thin force sensors of today (yellow) which need wires to sense (green) (b) Shows a possible integration of existing sensors with today's wireless technology, which end up making the sensing unit bulky because of electronics and battery requirements (green) (c) Shows ForceSticker's approach of using minimal electronics for digital identity whereas re-casting the popular capacitive force sensors to create analog force backscatter

sensor-devices bulky due to the need for batteries to power the ADCs and RFICs. Additionally, the use of batteries may not be practical for in-vivo applications as they can be toxic when placed inside the body. To overcome these challenges, it is important to develop low-power electronics for wireless sensor-devices, so that they can operate without batteries by using alternative power sources such as energy harvesting.

- **R4. Rapid deployment and Ease of usability:** Hence, there has been significant progress in the past decade in developing low-power RFICs for wireless sensor devices. One approach that has gained popularity is using the concept of "backscatter," which allows data to be transmitted by reflecting existing signals. However, this approach often requires new RFIC designs [21–23] or new reader devices to decode the backscattered data [24–26]. To facilitate rapid deployment and ease of use, it would be beneficial to make low-power wireless sensor devices compatible with commercially-available wireless technologies. This would enable use of matured, standardized protocols and eliminate the need for new RFIC designs and new protocol designs. Additionally, it would also allow for the use of commercially-available reader devices that have already approvals from regulatory authorities like FCC.

In summary, existing works fail to meet all these requirements, since, existing miniaturized force sensor-devices which meet R1, violate R2 as they require wired links to reader [10–13]. To achieve R2, and make wireless force sensor-devices, simple methods of data transmission over Wi-Fi/Bluetooth end up requiring batteries and violate R3 [27–30]. Now, to achieve R1, R2, R3 together, we can connect these sensors to a specialized low-power backscatter technology [21, 25] which can use a energy harvester to power up the RFICs. However, there is either no commercialized RFIC, and/or a reader-device to decode the backscattered data, which violates R4.

In this paper, we present ForceSticker, which meets all these requirements to enable a batteryless low-power wireless sensor-device with minimal electronics (Fig. 2c). Further, the wireless sensor-device is as thin as a paper and flexible, allowing it to conform to any irregular surface, akin to a sticker (Fig. 1(a-d)). As a consequence, ForceSticker can be simply stuck to any everyday objects to record the contact forces. These contact forces can take range from gravitational force (weight), to the joint impact forces sustained by orthopedic implants (Fig. 1d,e). The ForceSticker wireless sensor-device is composed of two main components: a thin and flexible mm-scale analog force sensor that transduces the applied force into wireless RF analog transformations, and a backscatter-based, battery-free commercial 900 MHz UHF RFID IC that provides a digital identity for these transformations. The RFIC interfaces directly with the sensor without the need for additional electronics, and its digital identity allows for easy readability with commercially available RFID readers utilizing mature EPC protocols. This makes ForceSticker sensors easily scalable and immediately deployable. We develop signal processing algorithms atop the commercial RFID readers to robustly extract the digital identity and analog RF transformations even in complex

multipath and reflection environments. Hence, the ForceSticker platform enables wireless force sensor-devices in a thin-flexible, sticker-like form factor, making them immediately usable for a wide range of applications.

The first component in ForceSticker wireless-sensor device is the mm-scale force-sensor which achieves zero power transduction. That is, the sensor by-itself transduces the force applied into measureable RF-analog transformations without requiring power. Essentially, the sensor transduces the applied force into measurable RF-analog transformations in wireless signals by simply utilizing small sub-mm deformations in a chosen polymer material. These deformations basically creates small capacitance changes, and this capacitance range is then tuned to create large, measurable RF-analog phase changes. This eliminates the need for additional electronics like ADCs or amplifiers for transduction, making the sensor zero-powered. Further, ForceSticker has developed a simulation platform in COMSOL to test and optimize choice of different polymer materials in the sensor to allow for easy customization of different force-ranges required for different applications.

The second component in the ForceSticker wireless sensor-device is the commercial RFID IC interfaced with the sensor. The RFID IC backscatters a fixed-unique identity signal in a battery-free fashion (wirelessly powered), which allows the sensor's RF phase transformations to be uniquely identified via this identity. Further, these RFID ICs are popular and commercially available, which also makes them immediately usable for variety of applications without any new RFIC development and commercialization. Now, to interface the RFID IC with ForceSticker, the key insight is to directly insert the analog RF phase transformations created by sensor in the wireless channel path of RFID tag (insert the sensor between the antenna and RFID tag). This in effect, creates a novel analog-digital backscatter communication, since the RFID tag has unique digital tag identity and its analog wireless channel has the force information. To achieve the sensor integration without loss in signal fidelity, the sensor interfacing is done with matched impedance co-planar waveguides. This integration of ForceSticker sensor with RFID IC does not reduce the readability range of the digital RFID; specifically the platform is tuned to create only analog-RF phase changes and not adversely affect the amplitude which may reduce the range. Hence, ForceSticker enables analog sensor data communication atop existing commercial RFID tags without degrading their reading ranges, which solves a challenging problem of RFID hacking to communicate sensor data [31].

Finally to enable ease of deployment, ForceSticker implements the required signal processing over a COTS RFID reader to isolate the analog sensor data from the measured RFID wireless channel. The RFID wireless channel consists of both sensor's analog channel alterations, as well as other wireless channel artefacts, like channel alterations caused by dynamically moving multipath in environment. We achieve this by leveraging the capability of COTS RFID readers to read phase changes over multiple RFID frequency channels. These phase readings over multiple RFID channels can be averaged to reduce the random-valued phase changes from the environment on each channel, while providing the averaging gain to the analog phase changes from the sensor which have a fixed value on each channel. This enables reliable wireless readout of applied forces on the mm-scale sensor in a variety of environments and even in the presence of moving objects in the environment. Hence, ForceSticker ushers in the vision of 'force-stickers' via the designed analog backscatter sensor piggybacked over RFID's digital identity, enabling wireless readout via a remotely located COTS RFID reader.

To summarize, we present the conceptualization, design and evaluation of a mm-scale wireless force sensor-device, ForceSticker. The developed ForceSticker device is thin and flexible, akin to a sticker, and is batteryless. ForceSticker's key idea to achieve this is to first design a mm-scale analog force sensor capable of transducing the applied force onto the RF analog phase changes. We prototype the sensor transduction based on the optimized capacitive range design from mathematical RF modelling, as well as perform multiphysics simulations in COMSOL to confirm the created model. The fabricated sensor by itself is 1000x lower volume form factor as compared to recent past work [32] on wireless backscatter force sensors. We integrate the sensor with popular RFID ICs, along with multiple different flexible antenna design which can be powered and read wirelessly with a standard COTS RFID reader. This interfacing of the analog phase force sensor and digital RFID IC allows wireless communication

of force via the analog phase changes created over the wireless channel characterized by the interfaced RFID IC's digital identity.

With ForceSticker framework, we design 4mm\*2mm sensor prototypes, with two different polymer layers of ecoflex and neoprene rubber, having force ranges of 0-6N and 0-40N respectively, with readout errors of 0.25, 1.6 N error each (<5% of max. force). Our experimental prototype shows results consistent with both our mathematical modelling and the multiphysics simulations in COMSOL. Further, we stress test ForceSticker by >10,000 force applications without significant error degradation. We test ForceSticker's wireless sensor-device to operate with ranges of ~ 5m over the air. Further, we test ForceSticker with challenging environments like, the sensor occluded via ~ 10 cm pork belly setup for in-body sensing, and people moving around the sensor-device to showcase the robustness of phase sensing to both reduced signal strengths, and dynamic multi-path. We also show a generalized sensor-design framework that could be used to develop sensors for different ranges of force, by choosing different polymer materials.

We leverage ForceSticker to conduct two experimental case studies by designing two different sensors for two diverse force ranges. In our first case study, we demonstrate reading different applied force levels on a toy-knee model to motivate the orthopaedic implant in-body application. Then, in our second case study, we put different quantities of objects in a package and read weight (gravitational force) via the force stickers stuck to the bottom of the package. By associating the read weight to number of items, we motivate a integrity check applications useful for warehouse measurement/smart checkout in grocery stores. ForceSticker's thin-sticker like form factor and flexibility, is also showcased in the supplementary demo video for weighing everyday objects and detecting knee-implant forces.

## 2 BACKGROUND AND MOTIVATION

In this section, we would first go over the four requirements (thin flexible form-factor, wireless readout, battery-free and immediate usability) in context of existing sensor devices, and explain briefly how ForceSticker achieves a wireless sensor-device which meets all these requirements. Then we will highlight the applications targeted by ForceSticker before going into design details of ForceSticker.

**Sensor devices meeting R1:** The existing commercial force sensors are typically MEMS-based discrete sensors that use a variety of transduction mechanisms, like the force-induced change of resistance/capacitance [10–13] and piezo current generated due to applied force [15–17]. These sensors by themselves are thin and flexible, (Meets R1, Section 1). However, they assume a wired connection to the reader-device, which violates wireless readout requirement (R2). An application where only R1 sensor-devices can be still useful is force sensors for trackpads, which requires a wired network of force-sensitive resistors [9, 33]. Since wired sensor readouts can easily be achieved via reader-devices being simple micro-controllers like arduino, these sensors typically also achieve R4.

**Sensor devices meeting R1+R2:** Now, in order to create a wireless sensor-device to meet R2, the device needs to have additional electronics like Analog to Digital Converters (ADCs) [34, 35] or Capacitance to Digital Converters (CDCs) [13, 36], as well as RF intergated circuits (RFICs) which then communicate the data across wirelessly. ADCs/CDCs and RFICs typically require battery to meet the power needs and hence this simple solution to create wireless sensor-devices violates R3 (battery-free operation). However, these sensors still work good for scenarios where R3 is not a stringent requirement, for example in latest AirPods for haptic-based volume control we have capacitive sensors [37], and some more force sensors under research for integration with wearable electronic devices like smart-watches [27, 28].

**Approaches which can potentially meet R1+R2+R3:** To make a low-power wireless sensor-device, one approach is to reduce the power requirements of RFIC by using backscatter which communicates data over reflected signals instead of generating a transmission of it's own. However, a challenge here is to make the



Table 1. Comparison of ForceSticker with prior batteryless works

Related Work	Meets R1? Thin/Flex.	Meets R2? Wireless	Meets R3? Batteryless	Meets R4? Immediate use	Demonstrated force sensor?	Applications/ Comments
<b>Unmousepad</b> [9]	Yes	No	No	Yes	Yes (Force sensitive resistors)	Force-sensitive trackpads
<b>Force sensors for wearables</b> [27, 28, 37]	Yes	Yes	No	Yes	Yes (Force sensitive capacitors/resistors)	Haptic control for air-pods, biomarker sensing
<b>uMedic</b> [25]+strain sensor [21]	Yes	Yes	Yes	No	No (strain sensor)	Can sense in-vivo organ elongations
<b>RF Band-aid</b> [24]	No	Yes	Yes	No	No (Temperature, Heart rate Breathing rate, Audio)	A general backscatter sensing platform
<b>WiForce</b> [32]	No	Yes	Yes	No	Yes (RF Transmission Line based sensor)	Able to detect and also localize forces
<b>RFID Hacking</b> [31] Mobicom'19 challenge paper	Yes	Yes	Yes	Yes	No (Temperature, Photointensity)	Sensor-RFID integration reduce readout range affect sensor accuracy
<b>This work</b>	Yes	Yes	Yes	Yes	Yes (Capacitive force sensors at RF frequencies)	In-vivo implants and ubiquitous weight sensing

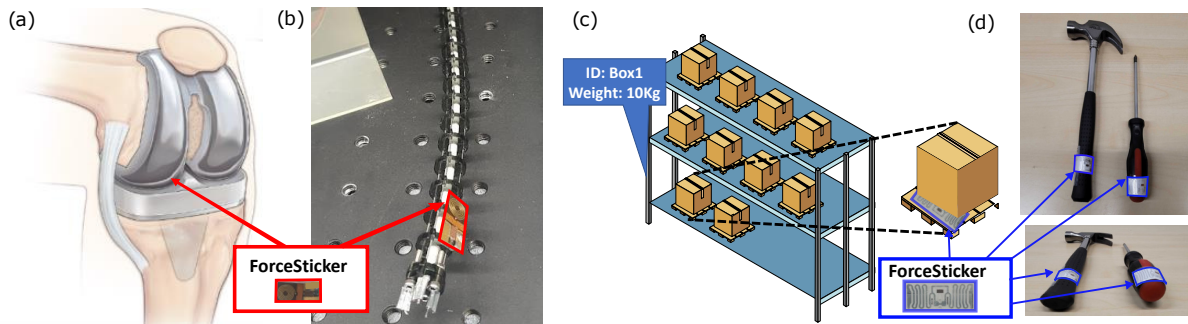


Fig. 3. (a-b) Show in-vivo applications of ForceSticker can be used for implant force sensing and and a possible integration of ForceSticker sensor with tendon driven surgical robots (c-d) Shows ubiquitous applications, how ForceSticker can be stuck on bottom of packages to measure the weight of contents inside for integrity checks, and how ForceSticker can be used to capture interaction forces from existing tools to allow for safe operation in industrial setting

interfacing electronics (ADC/CDC) low power enough that it can enable battery-free operations via energy harvesting. For example, a recent work integrates a commercial strain sensor and motivates usecases for in-vivo organ elongation sensing [21]. But the wireless readout range achieved by [21] is <30cm over the air and further it is not tested for in-vivo propagation environments. Aside from limited range, these sensor devices violate R4 as they are not immediately usable and require new RFID ICs designs that are not commercially available. Another work, [38] used a force sensitive resistor attached to a specific RFID IC, SL900A [39] which integrates an ADC with a RFID platform. However SL900A had a limited adoption, and is currently obsolete and not manufactured, hence violating R4 again. The reason for limited range, and less adoption of these platforms is because the sensor data digitization via ADCs is difficult to achieve with harvested energy. As a consequence, a large body of these digital sensor data backscattering platforms are battery-assisted[40–42].

An alternate approach which avoids ADCs altogether is to directly encode a resistive sensor onto frequency shifts using a resistor set oscillator [24]. However, this sensor platform was not used for contact force sensing, and was not shown to be fabricated in a miniaturized form factor since it requires bunch of discrete electronic

components not integrated in a IC form factor. Hence the demonstrated prototype ends up violating R1. Also, there is no commercial reader-device which can decode the backscattered frequency shifts, and as a consequence [24] uses a SDR reader instead of a commercial reader. Hence, [24] achieves R2+R3, while violating R1+R4. Another approach which bypasses ADCs was taken by [32], which designs an analog force sensor that encodes force readings onto wireless signal phases, and also uses frequency shifts as digital identity. However, similar to [24], it fails to meet R1+R4, while meeting R2+R3, since the sensor designed is not flexible as well as can not be miniaturized, and also requires a SDR readout to decode the frequency shifts.

**How to achieve R1+R2+R3+R4?:** One way of achieving R1+R2+R3+R4 could be to somehow figure out a wireless sensor-device with RFIDs. Today, RFIDs are available popularly (meets R4), and already come in sticker like form-factors (meets R1 independent of force sensor) and are capable of communicating to a remotely located RFID reader (>3m typically) without any battery by relying on energy harvested via RF signals (meets R3). The only missing tool is to somehow figure out how to perform sensor's wireless readout with RFIDs (R2) since today's popular RFID stickers lack interfacing electronics like ADCs required typically by existing sensor-devices. Hence, the challenge here is how to hack the popularly available RFID platform into communicating not just communicate the RFID's digital identity and, but the sensor data as well.

Here, ForceSticker has a key-insight of piggybacking the sensor's analog data over the RFID's digital identity. That is, since the remotely located reader is able to detect signals from the RFID because of its unique digital identity, it can estimate the wireless channel between the reader and RFID. Hence, if we can somehow interface the sensor to create analog changes in this RFID-reader wireless channel we can communicate analog data via changes in channel state computed over the RFID's digital identity. This approach has also been supported by an initial direction [31] which tried directly connecting COTS sensors to RFID by cutting a small part of the RFID antenna and replacing it with the sensors in series. [31] evaluates this strategy for Temperature/Light sensors where the sensors impedance changes due to a change in Temperature/Light, similar to how force sensors change impedance under forces. This change in impedance across the cut parts of antenna creates fluctuations in the wake-up thresholds of the energy harvester, and this fluctuation is used as a metric for wireless sensing. However, this technique hampers the RFID read range in the process as it disturbs the energy harvester, which impacts the quality of the reflected signal and hence the sensor resolution. In fact, this particular past work [31] poses the sensor integration with RFIDs as a 'challenge paper', so as to how to integrate the sensors without losing range and resolution in the process.

Hence, ForceSticker also gives a possible solution to the RFID sensor data communication 'challenge'. ForceSticker designs a new miniaturized force sensor that works as a capacitive sensor, which brings about analog backscattered phase changes when interfaced in parallel connection (shunt mode) between the RFID IC and the RFID antenna. At the same time, this shunt capacitor interfacing allows passing of signals through the RFID IC and hence obtains digital identity atop the created analog phase changes. This basically creates phase shifts in the wireless channel between the reader-device and RFID. Further, the capacitor creates only minimal changes in amplitude by affecting only the signal phase, and hence it preserves the range of the RFIDs. This allows the RFID reader to sense with highest signal fidelity and hence obtain the highest possible resolution. Due to this successful analog data integration over digital RFIDs, we achieve the first wireless force sensor-device in a sticker-like form factor, which meet R1+R2+R3+R4.

This discussion so far on different sensor devices, and their applications is also tabulated in Table 1.

**What applications get enabled when we meet R1+R2+R3+R4?** The main applications targeted by ForceSticker can be broadly divided into two categories: in-vivo applications (orthopaedic implants and surgical robots) and ubiquitous sensing (weight sensing and contact forces due to human-tool interactions), as depicted in Fig. 3.

For in-vivo applications, like knee-implant based force sensing [43–45] to characterize implant health, and surgical robot force sensing for safer surgeries[46–48], the core-requirements from force sensors are flexible and thin form-factor, wireless readout and battery-free operation (R1+R2+R3 in Section 1). Although one can argue

to create a specialized platform for such applications, which may not be immediately usable (R4), it limits the available experimentation and adoption of such solutions. The case being, since ForceSticker uses commercially available RFID ICs and readers, instead of requiring a new design, ForceSticker is capable of running large-scale field trials and show feasibility of such battery-free platforms for medical usecases.

For ubiquitous applications involving sensing of weight and interaction forces, main requirements are flexible and thin form-factor, wireless readout and immediate usability (R1+R2+R4 in Section 1). Here, one can argue that going battery-less (R3) is strictly not needed, as these applications can use a battery backed sensor. However, again, requirement of batteries limits both adoption, as well as the required cost and environmental footprint [49]. Batteries need to be replaced often, and are difficult to decompose and contribute largely to the embedded carbon footprint. ForceSticker's simple sticker-like design is far-more intuitive and can be used across multiple such applications without requiring complex battery integrations. ForceSticker can basically enable RFID barcodes which can be read wirelessly and also give the weight of the object in addition to the identity (Fig. 3c). This can be very useful in a warehouse scenario where an operator can simply walk by bunch of packages, scan their RFID barcodes and immediately know their weights which can later be used for integrity checks [50, 51].

Next, these sensors can also be stuck to everyday tools and be used to measure the interaction forces as one operates the tools. In an industrial scenario, this can be useful to determine safe operation of such tools and identify failure cases easily (say one used a high impact force with a hammer which broke an object). Instead of requiring sophisticated tools with embedded sensors inside, requiring charging and/or battery replacements, ForceSticker can simply be stuck on common everyday tools and make the tools force-sensitive. For ubiquitous applications, such stickers can enable plethora of previously unthought-of applications, by augmenting everyday objects with a sticker-like force sensor, for example sticking the sensor on a chair to sense sitting posture and forces, or sticking them on simple everyday objects like water bottles/milk cans to weigh their contents.

### 3 DESIGN

ForceSticker presents the first sticker-like, wireless, and batteryless (mm-scale) force sensor-device. In this section, we delineate various facets behind ForceSticker. First, we will present the capacitance to RF phase transduction mechanism, which allows ForceSticker mm-scale sensor to transduce applied force onto measurable analog-changes in the backscattered RF signal. Going ahead, we show how to interface the designed sensor with RFID ICs to provide a discernible digital identity to the sensor's phase shifted signals. Finally, we present the details on how an externally located RFID reader decodes the analog phase shifted signal over the digital RFID to successfully measure the applied forces on the wireless batteryless sensor-device.

#### 3.1 Encoding Force onto Analog Changes in the Backscattered Signals from the mm-scale Sensors

The first design component in ForceSticker is the design of the analog force sensor which directly transduces the applied force onto RF signal transformations. These analog transformations can then be carried over the wireless channel of the digital RFID. Now, the available quantities to create these analog transformations are the amplitude, polarization or phase of the RF signals. Since the sensor is batteryless, it can not increase the amplitude of reflected signals, but it can reduce the amplitude based on applied force. The reader can associate this force-dependent amplitude reduction to the applied forces. However, this also entails reduced range, since the sensor is adversely affecting the already weak backscattered signal and reduces reading range, as well as signal fidelity of RFID, as also observed in past related work [31]. Hence, it is desirable that sensor doesn't adversely affect the amplitude, but try to encode changes in polarization/phase. However, changes in polarization are difficult to sense, since polarization angles are reported by very few platforms as of now. In comparison, phase readings are reported by many COTS RFID readers, has been shown to be robust to enable analog sensing in prior work [32, 52, 53], and does not adversely affect the signal amplitude.



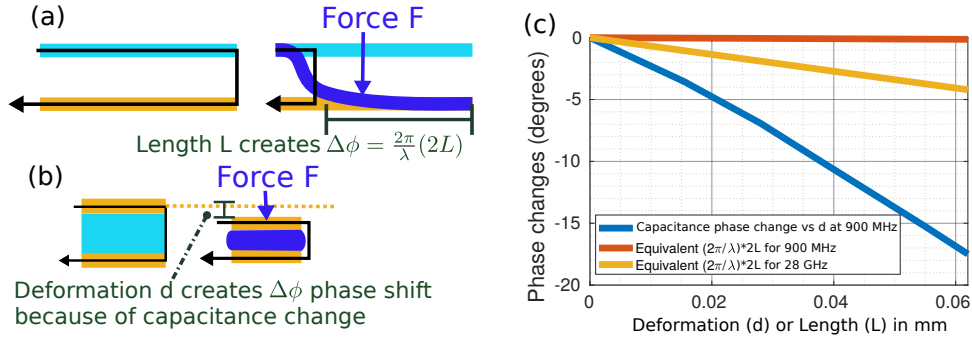


Fig. 4. (a-b) Shows a visual comparison between ForceSticker’s capacitive transduction mechanism and past work’s [32] length based mechanism (c) Shows how the capacitive phase transduction mechanism allows for sensor miniaturization with measurable phase changes even when deformations are sub-mm scale

However, creating measurable and practical phase changes is challenging for mm-scale sensors. The reason is that phase is most commonly associated with length of signals travelled, with the most popular phase equation being  $\phi(d) = \frac{2\pi}{\lambda}d$ ,  $\phi$  is the accumulated phase and  $d$  is the distance travelled by the wireless signal having certain wavelength  $\lambda$ . Hence, to accumulate substantial measurable phase, the distance travelled has to be in order of wavelength, for practical sub-6 GHz wireless signals, this computes to  $<10\text{cm}$ , which doesn’t allow for mm-scale sensor [54, 55]. This is also observed with the past-work, WiForce [32] sensor (Fig. 4 (a)), which was a 8 cm long sensor to capture measurable phase changes at 900 MHz frequency. If the sensor is hypothetically miniaturized to mm-scale with sub-mm deformations, the net change in phase would be  $<1^\circ$ . Even if the sensor design is scaled to higher frequencies like 28 GHz, it will fail to give measurable phase shifts of  $> 10^\circ$  (Fig. 4 (c)). Worse yet, the presence of an air gap in ForceSticker design to allow for bending effects makes the design impossible to create in a thin sticker-like form factor even if the length is somehow miniaturized successfully.

ForceSticker designs a new way of creating phase shifts, instead of the traditional distance based methods. This paves the way to miniaturization of sensors, as well as create an easier abstraction to allow for more intuitive sensor designs. The core idea is to simply sandwich a soft polymer layer between two conductive layers which creates a parallel plate capacitor. Under effect of force, the polymer layer would deform and the conductive layers will get closer, which would increase the capacitance (Fig. 4b). Now, when this sensor is connected to an antenna which received the RF signals, the change in capacitance affects the reflection boundary conditions, and creates the phase changes in effect. Fundamentally, when we go to this new transduction mechanism of capacitance to phase, we associate phase changes due to sensor thickness deformations instead of sensor length deformations. Hence, this transduction mechanism does not depend on the sensor length and instead depends on sensor thickness, thus allowing the sensor to be made with very small length form factors.

Further, this relationship allows creation of paper-like thin sensors, since unlike the linear phase to length relationship, the relation between the thickness deformation and phase change is non-linear. As a consequence, the non-linear relationship can be exploited to operate in a ‘sensitive’ region where measurable phase changes are obtained even when the thickness only changes by 0.06mm, which is even lesser than a typical thickness of paper strip of around 0.1mm (Fig. 4c). Hence, with this new transduction mechanism, we can create sensors which are about same thickness as a paper strip and hence are sticker-like form factor. In the next section, we will explain how to model this non-linear phase to capacitance relationship mathematically, and harness this mathematical model to design the mm-scale ForceSticker. Further, we also verify this mathematical model via multi-physics simulations.

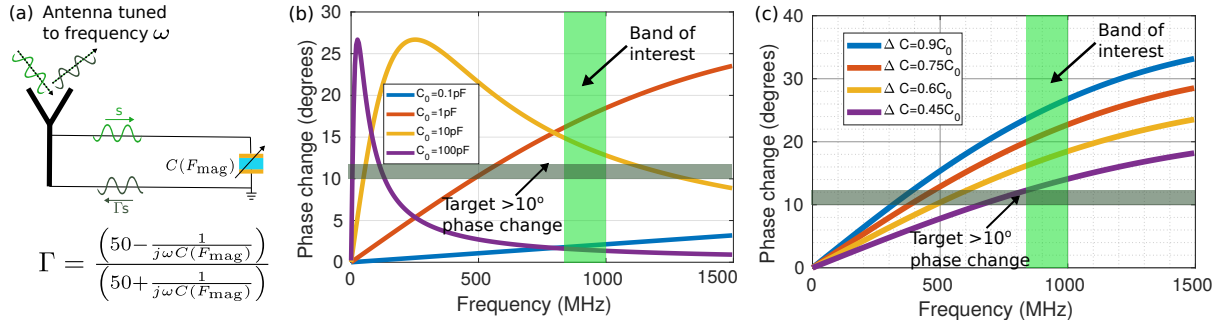


Fig. 5. (a) Reflection coefficient equation (b) How different values of  $C_0$  affect  $\Delta\phi$ , plotted at a constant  $\Delta C = 0.75C_0$  (c) How different  $\Delta C$  affect maximum phase shift attainable, plotted at constant  $C_0 = 1$  pF

### 3.2 Mathematical Modelling, Multiphysics Simulation of mm-scale Capacitive Force Sensors

Because of the non-linear relationship between capacitance and phase change, the capacitive sensor has to be designed to operate in a 'sensitive' range, where the phase shifts are large and measurable. Further, we need to tune the capacitance value such that the non-linear equation sensitivity is exploited in the desired frequency band of 900 MHz for the commercial UHF RFIDs. To obtain this sensitivity tuning, the capacitor needs to have a correctly designed 'nominal value' at zero force, denoted by  $C(F = 0)$ , denoted as  $C_0$ .  $C_0$  basically governs if the sensor's phase change is sensitive to a chosen RF frequency  $\omega$ , and the non-linear relationship is given as:

$$\Delta\phi(F_{\text{mag}}) = 2\tan^{-1}(1/50\omega C(F = F_{\text{mag}})) - 2\tan^{-1}(1/50\omega C_0) \quad (1)$$

where  $\Delta\phi(F_{\text{mag}})$  is the phase change brought by  $F_{\text{mag}}$  force which creates  $C(F_{\text{mag}})$  capacitance. Due to presence of  $\tan^{-1}$ , the phase to capacitance is not a simple linear relationship unlike the phase to distance relation before. This non-linear relationship is derived from reflection coefficient calculations  $\Gamma$ , assuming a transmission line matched to 50 Ω as shown in Fig. 5 (a). Basically, the reflected signals from the capacitor are multiplied by the reflection coefficient  $\Gamma$  and then backscattered by the antenna. Due to the purely capacitive nature of the sensor impedance,  $\Gamma$  has the form of  $\frac{a-bj}{a+bj}$  and hence can be rewritten in polar form as  $\frac{\sqrt{a^2+b^2}e^{-j\tan^{-1}(b/a)}}{\sqrt{a^2+b^2}e^{j\tan^{-1}(b/a)}}$ . Thus,  $\Gamma$  has unit magnitude and a phase term given by  $2\tan^{-1}(b/a)$ , and hence the phase change computes to the non-linear relationship specified in Eq. 1.

Hence to utilize the non-linear relationship and get the best sensitivity, we need to tune  $C_0$  such that  $\Delta\phi$  is maximized for the operating frequency  $\omega$  (Fig. 5b). Intuitively what is happening in Fig. 5b is that Eq. 1 has the arctan function, which saturates as the input gets closer to both 0 and  $\infty$ , and hence at  $\omega \rightarrow 0$ , the total phase changes are negligible as the input is driven to  $\infty$  and at high  $C_0\omega \rightarrow \infty$  the input goes to 0 and that also gives lesser phase changes. A second variable which governs the best possible phase shift attainable, is  $\Delta C = C(F_{\text{max}}) - C_0$ , where  $F_{\text{max}}$  is the maximum force sustained by the soft layer (Fig. 5c). Basically, if there is lesser capacitance change, there is lesser phase change at all frequencies. Hence,  $\Delta C$  variable doesn't have effect on frequency, but just on what is the maximum phase change which can be attained at a particular frequency tuned by  $C_0$ . Hence, these two variables  $C_0, \Delta C$  govern the phase change mechanics given by the non-linear relation in Eq. 1.

We show as an example on how to design sensors tuned to 900 MHz. From Fig. 5 b,c, we observe clear targets that  $C_0$  needs to be between 1 – 10 pF and  $\Delta C$  needs to be greater than  $0.45C_0$ . Nominal capacitances can be approximated to be  $C = \frac{A\epsilon_r}{d}$  as under no force the sensor is essentially like a parallel plate capacitor, with a Ecoflex

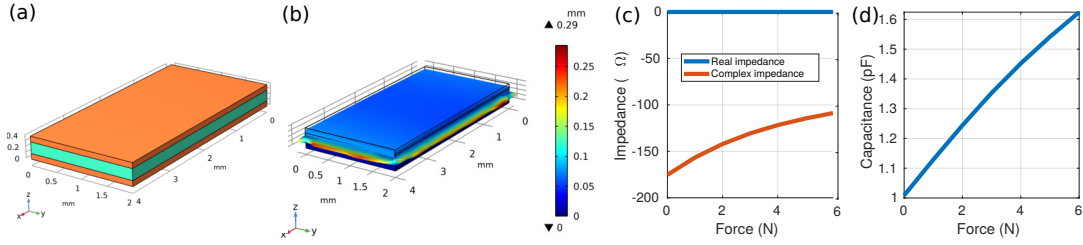


Fig. 6. (a) Sensor mechanical composition (b) Deformation under action of force (c) Sensor impedance (real, complex) vs Force (d) Capacitance versus Force simulations

00-30 polymer dielectric layer sandwiched between two copper layers (Fig. 6(a)). The choice of dimensions of the sensor gives a rough initial capacitance of  $1pF$ , with  $C = \frac{A\epsilon_r\epsilon_0}{d} = \frac{8*10^{-6}*2.8*8.85*10^{-12}}{0.2*10^{-3}} = 0.99pF$ , with a  $2mm \times 4mm = 8mm^2$  area sensor with  $0.2mm$  thick dielectric layer, and the dielectric constant =  $2.8$  for the chosen Ecoflex 00-30 polymer [56].

Unlike the parallel plate approximation of  $C_0$ ,  $\Delta C$  does not have a close form expression as it requires calculation of the mechanical deformations caused by force. Additionally, the sensor geometry under force is not as simple and becomes that of a squished polymer layer (Fig. 6 a,b), which affects capacitance calculations. Hence,  $\Delta C$  computation requires solving both the structural mechanics equations to compute the polymer deformation and then use the deformed geometry for maxwell equations to compute the effective capacitance of the squished sensor. As this is not analytically straightforward, we utilize a FEM simulation framework, COMSOL Multiphysics 6.0 [57], to simulate the sensor capacitive effect under deformation.

COMSOL takes the sensor geometry as an input and meshes the geometry to form small elements where the differential equations can be solved numerically, and the final results are then collated across each mesh element's solution. We use COMSOL Structural Mechanics module for the non-linear elastic modeling of the polymer layer and via COMSOL AC/DC module, we can excite the sensor with an AC voltage source and compute the obtained current as affected. This computation can be done with the sensor being under the effect of various levels of force applied to the sensor. Then, by simply taking voltage to current ratio we can obtain the sensor impedance as a function of force,  $Z(F_{mag}) = V(F_{mag})/I(F_{mag})$ . Hence, this allows the computation of sensor impedance versus force readings (Fig. 6c). Since the resistive component of the impedance is almost 0, and the reactive component is negative, it shows that the sensor is almost purely capacitive. We obtain the capacitance to force curve as shown in Fig. 6d, with the observed capacitance of the ecoflex sensor going from 1 to 1.65 pF as the force on the sensor increases from 0 to 6 N. This meets our target of sensor design with the nominal capacitance of about 1 pF and  $\Delta C = 0.65C_0 > 0.45C_0$ .

### 3.3 Providing Digital Identity to the Capacitive Sensor for Robust Wireless Readout

For the wireless readout of the sensor in a practical environment with multipath, it is not enough to just create analog phase shifts in the backscattered reflected channel. In an anechoic chamber assuming only the reader and the sensor, we can read the analog phase changes directly from the sensor reflected signal. However, in a realistic environment, there would be myriad of environmental reflections in addition to sensor reflected signal at the reader. In order to read the reflected signal phases from the sensor, it also needs to isolate the sensor reflections from the myriad of environmental reflections. Hence, it is required for the sensor phase-shifted signals also to somehow have a digitally-readable identity to distinguish the sensor signal from the environmental reflections. The challenge here would be how can we add the digital identity in an immediately usable batteryless manner?

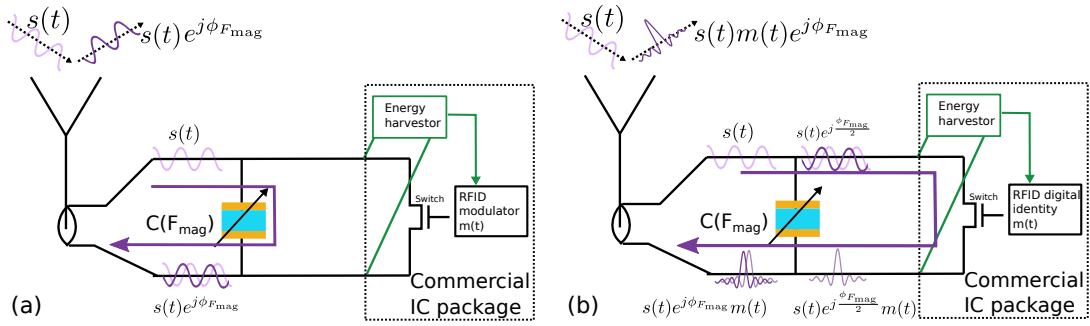


Fig. 7. Interfacing the analog capacitive sensor with digitally identified RFIDs, by inserting the sensor in between the antenna and RFID IC connected in parallel to both. (a) shows what could be a degenerate solution to reflection equation, but capacitive phase transduction doesn't work this way (b) shows the actual mode of operation of the capacitive transduction

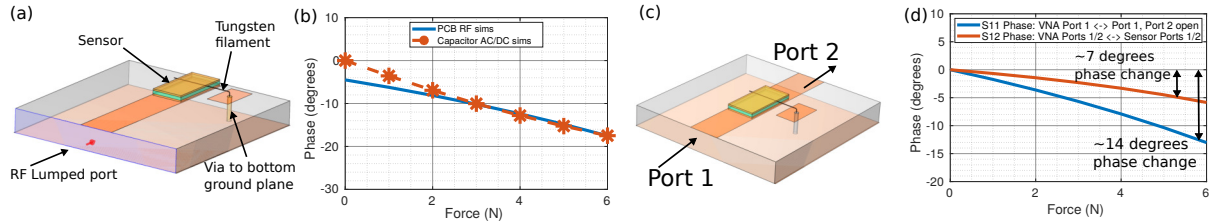


Fig. 8. (a) PCB sims with RF module (b) Phase change from RF simulations (blue) are well modelled by the extrapolations from AC/DC simulations (red) (c) Simulating sensor in thru mode (d) Phase doubling effect in simulations

An attractive option is to use RFIDs to provide digital identities. RFIDs use energy harvested from RF signals to create on-off digital signatures in the reflected signal which carry the digital identity in the signal. The technology has matured, and commercialized over the past decade, supported by scalable EPC protocol [58] and commercial tag readers. There are other ways of creating a digital identity, for example, creating identity based on freq. shifts [24, 32], but these methods are not in an immediately usable IC form factor and can not build atop of years' of research gone already into RFID. Hence, ForceSticker proceeds to adopt RFIDs as a method of providing digital identity, while enjoying benefits of a IC form factor and matured RFID protocols.

While interfacing an RFID IC, it is required that sensor be placed in between the antenna and RFID IC, since the RFID IC is a single port device and does not pass the signals through. However, with the sensor characterization done so far, there are two degenerate solutions. First one as shown in Fig. 7a assumes that all the phase change is directly reflected off the sensor with no signals reaching the RFID block. The second one (Fig. 7b) assumes that the sensor passes the signals through as well as give the phase changes, and thus can work with the RFID IC. We show that the Fig. 7a actually doesn't happen in reality, and the sensor in fact provides phase changes even in a thru mode as shown in Fig. 7b. This phenomenon of force induced capacitive thru-phase change, draws a parallel to varactor-based RF phase shifters popular in antenna arrays. Varactors are basically small voltage tunable capacitors and produce a similar programmable thru-phase shift depending on the supplied voltage [59]. The exact mathematical modelling of this effect is out of scope of this paper, but can be found in varactor literature [60]. Instead of the mathematical model, we showcase the sensor's working in thru mode via RF level simulations, which allows the sensor to be integrated easily with RFID ICs.

In order to simulate the thru-mode responses of the sensor in hardware, we perform 2-port simulations in COMSOL with the sensor interfaced on a PCB which implements a  $50\Omega$  transmission line. In section 4, we further fabricate this PCB to confirm the sensor's thru-mode response with actual hardware measurements. In a way, this PCB practically implements our capacitive sensing motivation Fig. 5a. The PCB consists of two layers; on the top, there is a signal trace which is 2 mm wide, similar to the sensor, and the bottom layer is the ground plane. The bottom copper plate of the sensor is directly soldered onto the signal trace. Now, in order to have the sensor and PCB ground common, we use a  $20\mu\text{m}$  tungsten wire filament to connect the top copper plate with a small ground pad on the top layer using a via (Fig. 8a). The sensor is excited via a lumped port at the other end of PCB. This simulation using the COMSOL RF module is then linked to the COMSOL Structural Mechanics module to compute the deformations with the updated sensor with the tungsten filament. With this linkage, the multiphysics simulation calculates the capacitance change from the structural deformations, as well as calculation of the phase from the capacitor's scattering parameters. Hence, this RF+Structural Mechanics multiphysics model allows simulation of the force induced phase change effect for the sensor+PCB+tungsten wire platform.

We confirm that the S11 phase changes (about  $20^\circ$  from RF COMSOL simulations) from the RF module simulations are consistent with the earlier simpler simulations with AC/DC module (Fig. 8b). Note that the AC/DC module just give capacitance measurements which are mathematically converted to phase via Eq (1), whereas the RF module simulation is a faithful end-to-end FEM simulation which confirms that the sensor can work in a practically manufacturable manner and physical lumped ports. The small discrepancies can be attributed to two facts. First, the AC/DC module computes capacitance at small AC frequencies (a few kHz), which may not be purely accurate at 900 MHz. Further, the addition of small tungsten filament may also cause some additional minor discrepancies.

Now, by moving the sensor to the middle of the PCB in these simulations (Fig. 8c) compared to towards the end, as shown previously (Fig. 8a), we also confirm working of sensor in a thru-mode. This allows us to define two lumped ports (Port 1, Port 2), one on each end of the PCB, and by observing the S12 phase, we can verify if the sensor can work in a thru mode. For this simulation, we obtain the S12 phase changes and observe that the phase changes are about half the magnitude we had before, that is  $10^\circ$  for 0-6 N forces as compared to  $20^\circ$  before. Now, when we keep the other port as reflective and estimate the S11 phase, we get almost the same phase shifts as before (around  $20^\circ$ ). This thru-mode simulation finally leads to a complete understanding of the sensor's RF level interfacing.

Hence, intuitively what happens is that when a signal  $s(t)$  travels through the sensor, it first gets a certain value of phase shift and the sensor passes the signal through  $s(t)e^{j\phi(F_{\text{mag}})/2}$ . Then, when the signals get modulated  $s(t)e^{j\phi(F_{\text{mag}})/2}m(t)$ , reflect and pass through the sensor again, the total phase shift doubles up  $s(t)e^{j\phi(F_{\text{mag}})}m(t)$  and reaches back to the reflective levels as described in Eq. (1), as visually illustrated in Fig. 7. Thus, the reflected signal has both the identity component from the RFID IC as well as a phase shift. The RFID reader can use the RFID IC's digital identity to isolate the sensor reflections from the environmental reflections and then estimate these phase shifts from channel estimation done on the isolated signal.

### 3.4 Putting It All Together: Reading Forces (Phase Shifts) via COTS RFID Readers

To tie up ForceSticker's design, the only component left to describe is the wireless reader. As explained towards the end of the previous subsection, when ForceSticker sensor is interfaced with RFID, it reflects back a digital identifiable phase-shifted signal. The digital identity from the sensor is given via the EPC ID number of the RFID IC integrated with the sensor. Then, the RFID reader can observe the channel estimates of the particular tag given by the EPC id and calculate sensor phase jumps to estimate applied forces.

However, in order to estimate these phase jumps with COTS readers, a challenge is make the phase sensing robust to the hopping nature of these COTS readers [52, 61]. As per FCC guidelines, the readers need to change



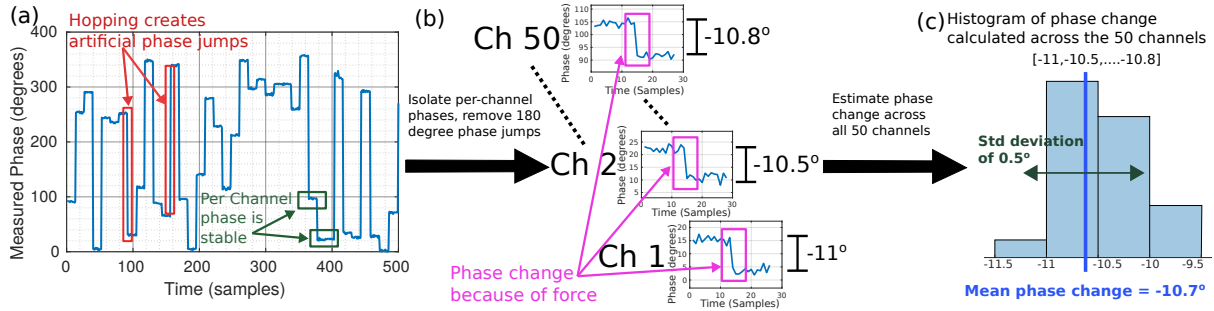


Fig. 9. Computing phase change resulting from force applied on the analog capacitive sensor: (a) Shows raw phases from RFID reader (b) Shows per channel phases, by taking differential phase per channel the fixed hopping phases are suppressed and (c) Finally shows how phase jumps are consistent across all the channels

their frequencies after every 200 milliseconds to avoid interference with other readers in the environment. The COTS readers introduce a random phase offset due to hopping, as the PLL locks to a different frequency, and this inadvertently shows up as phase jumps in the phase calculations. However, using the Low Level Reader Protocol (LLRP) for RFID readers [62], we can isolate the per channel phases since the COTS readers give a channel index for each phase readings, and the phases on a particular channel remain stable across time and do not show these jumps [61]. Hence, this allows ForceSticker to compute differential phase jumps per channel, which computes the phase shift value caused by force per channel. Using differential phase automatically offsets the fixed phase jumps across channels and gives a consistent phase jump measured across multiple RFID channels. In addition to hopping-based phase jumps, the Impinj RFID reader used has phase readings which show  $180^\circ$  shifts and we handle this in our implementation by detecting the phase jumps  $> 170^\circ$  and removing this  $180^\circ$  appropriately. Since the force information is encoded in phase jumps which does not exceed jump magnitude of  $20^\circ$ , we can always detect higher than  $170^\circ$  jumps and attribute those to Impinj reader's flaw than force and hence obtain clean jump free phases per RFID channel from the reader. Then, we can further average the phase jumps recorded across each of the 50 RFID channels between 900-930 MHz to get clean phase jump readings from the RFID reader. This whole process is visually illustrated in Fig. 9.

A unique insight ForceSticker has on this RFID sensing is that such multi-channel RFID phase averaging makes the sensing robust to dynamic environmental multipath since each channel records different phase jumps stemming from the dynamic multipath because of its moving nature. However, the phase jump from the sensor remains consistent across the channels. Thus, upon doing multi-channel averaging across these 50 distinct channels, the multipath phase jumps get averaged out to near zero, and the sensor phase jump remains at its consistent level. Further, the dynamic multipath phases being different across different RFID channels allows us to remove fake positive phase changes by profiling the standard deviation of phase changes observed across multiple channels. A phase shift from dynamic multipath would show large standard deviation across the channels as compared to that from force sensor. Hence, as seen from the supplemental video, the averaged and filtered phase changes do not fluctuate due to hand lifting and placing the weight.

From our experiments, we have observed that in a static environment, such averaging gives phase measurement accurate to  $0.5^\circ$  in static scenarios which leads to a sensor resolution of  $0.2N$  (Since  $0-6N$  shows approximately  $0 - 15^\circ$  phase jump and hence resolution would be  $\frac{6}{15} * 0.5 = 0.2N$ ). When there is dynamic movement in the environment, the measurements are roughly accurate to  $0.8 - 1^\circ$  (depending on extent of movement) which makes the resolution slightly higher to  $\sim 0.3 - 0.4N$  which is still at sub- $N$  levels. Further,  $0.3N$  is also the reported resolution of forces felt via our fingertips in HCI research [63], and hence, good enough for many realistic

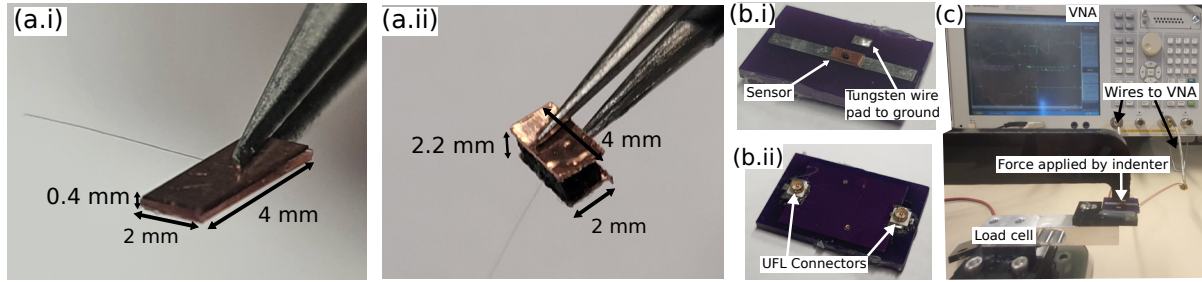


Fig. 10. (a) ForceSticker’s analog sensor with (i) ecoflex polymer and (ii) neoprene polymer and the tungsten wire filament (b) Sensor interfaced in parallel to a microstrip line implemented on a PCB, with (i) showing top layer (ii) bottom layer (c) shows the setup to perform wired test at RF frequencies: with forces being applied by an actuated indenter, and ground truth forces measured by the load cell and phases captured by the VNA connected to the PCB via the UFL connectors

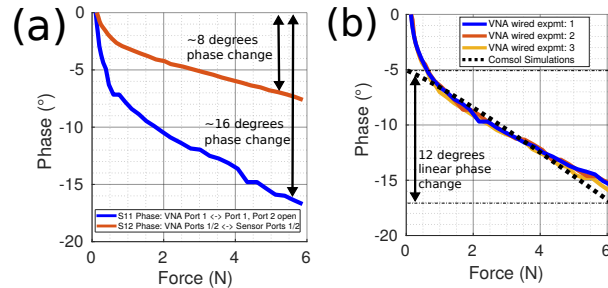


Fig. 11. (a) Shows S11 and S21 phase to force profiles of the analog capacitive sensor, measured via ForceSticker’s rigid PCB test platform connected to VNA and (b) Shows sensor consistency over multiple trials and with COMSOL simulations

applications. Hence, ForceSticker calculates the phase jumps at each of the RFID hopping frequencies and then averages them to obtain a very clean phase jump measurement (to about  $0.5 - 1^\circ$  precision) which can then be used to compute multiple force levels within the net  $15^\circ$  phase jump given by the sensor, with achievable resolution reaching to sub-N levels of  $0.2 - 0.4N$  across various environmental scenarios.

## 4 IMPLEMENTATION

In this section, we briefly describe sensor-device implementation, including how to fabricate the analog sensor, the flexible PCB and custom designed small antenna version of ForceSticker, and also a PCB-free method of interfacing with commercial RFID ICs. To conclude the section, we present details on the signal processing done atop COTS RFID reader to calculate the forces from the sensor.

### 4.1 Fabrication of the Capacitive Force Sensor Which Transduces Force onto RF Phase Changes

The first component in the ForceSticker implementation is a capacitive-based force sensor which provides analog phase shifts at RF frequencies. The sensor design basically mimics a parallel plate capacitor, and thus consists of three layers: a conductive metal layer at the top and the bottom and a dielectric polymer layer in the middle. To fabricate the sensors,  $0.1$  mm copper strips are used as conducting layer. Depending on the maximum force to be read, the soft polymer can be either Ecoflex-0030 elastomer ( $<6N$ ), Neoprene 30A rubber ( $<40N$ ) or carbon filled black rubber ( $<600N$ ). We fabricate the ecoflex and neoprene sensors with the thickness being  $0.2$  mm and

2.2mm each, whereas the carbon filled rubber sensor is only in simulations. The thickness of rubber sensors is higher since these have higher dielectric constants [64], hence to keep similar area form factor the thickness has to increase (but still remains mm-scale). These dimensions are estimated as per the capacitive tuning model discussed in Section 3.1 to provide measurable analog phase shifts at 900 MHz.

In order to fabricate the ecoflex layer, we utilize a blade coating process to get 0.2 mm thick uniform, which then can be cut into a 2 mm × 4 mm piece for the sensor. For more details on the ecoflex layer fabrication process, please refer to [65]. Neoprene rubber is commercially available as 2mm thick layer, which can then be laser cut into the 2 mm × 4 mm form factor. The copper plates are then stuck onto either side of the fabricated polymer layers. Before bounding the top side of the polymer layer, a commercially available tungsten wire filament [66] with 20 μm diameter is placed on the polymer layer, so that the top layer can be electrically grounded to interface the capacitor in parallel to the RFID IC. The filaments are also flexible and bendable as a consequence of μm form factor and can be twisted and flexed akin to human hairs. A zoomed-in image of the fabricated sensors are shown in Fig. 10(a.i), (a.ii).

#### 4.2 Experimental Verification of RF Analog Phase Changes from mm-scale Sensor via RF PCBs

Now, we describe how we interface sensors on RF PCBs to experimentally confirm the simulation results presented in Section 3. To implement the transmission line PCB, we design a microstrip line of 50 Ω impedance at 900 MHz, that has a width of 2 mm so that the sensor can be directly soldered on it (see Fig. 10 b.i). The PCB that supports the microstrip line also has a small ground pad for soldering the tungsten wire filament. The signal traces are taken to the bottom layer using vias, where the line is terminated in two UFL connector pads (Fig. 10 b.ii). Using this PCB we can interface the sensor via RF cables to a VNA (Vector Network Analyser), a measurement device which mimics a wireless transmitter by exciting the sensor with 900 MHz signals and observing the reflected and transmitted signals, hence providing wired ground truth phase measurements. Further, we mount this sensor PCB on a load cell sensor, in order to have ground truth force measurements. For ground truth characterization, we apply forces on the sensor via an actuator. The RF cables connect the VNA ports to the PCB UFL connectors on the bottom side of the PCB (Fig. 10c). The placement of the UFL connectors on the bottom side of the sensor allows the actuator to apply forces on the top surface of the sensor without creating mechanical hindrance.

In order to compare our physical prototype with our COMSOL simulations, we plot the force and phase measurements, shown in Fig. 11 (a-b) made by VNA in both reflect-mode (S11 measurements, Port 1 connected to VNA and Port 2 reflect open) and thru-mode (S21 measurements, both Ports 1,2 connected to VNA). Similar to our intuition as shown in Fig. 7 and COMSOL simulation results as shown in Fig. 8, we observe that the phase doubling effect happens in the physically prototyped PCBs as well (Fig. 11), since from the thru-mode to reflection-mode the phases double up from 8° phase shift to 16°. Also, we observe consistency with our COMSOL simulations, since both simulations and hardware results show about 12 degree linear phase change. However, there is a non-linear part for lower forces (< 1 N), which is common across capacitive sensors [67, 68] and can not be modeled accurately via COMSOL's numerical computations. We confirm that the non-linear response originates from the sensor, and is not an artefact from the PCB, since even the non-linear part doubles up from transmit to reflect mode, which is only possible if the phase originates from the sensor. This initial non-linear part is also repeatable across measurements, and in fact improves the sensor sensitivity in low force ranges. Further material characterization can be done in future and the COMSOL models can be improved in order to better model this non-linearity.

#### 4.3 RFID Integration with Sensor to Provide Digital Identity

Finally, having described how the capacitive sensor is fabricated and the hardware verification of the analog phase change effect, we show how the digital identity is provided to the sensor via RFIDs.

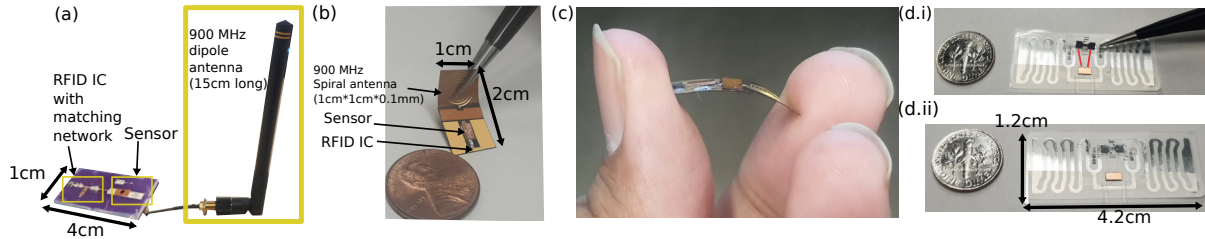


Fig. 12. Interfacing the capacitive sensor with RFID ICs: (a) Shows the ForceSticker test platform rigid PCB with matching network and dipole antenna (b) Shows ForceSticker’s spiral antenna flex PCB with a dime coin to scale (c) Shows the flexibility of the spiral antenna PCB and (d) Shows how ForceSticker peels the RFID IC from the antenna and attaches the sensor via two tungsten filaments (highlighted in red, d.i) to create the standalone RFID ForceSticker version (d.ii)

Proceeding in steps, we first extend the sensor PCB further and add a RFID IC [69] pad and a corresponding T matching network right after the sensor pad (Fig. 12a), in a way implementing the block-level diagram as shown in Fig. 7 on actual PCB hardware. With this PCB prototype, we can connect a simple dipole antenna to the UFL port and use it to interrogate the capacitive sensor+RFID platform wirelessly. The T matching network allows testing of different matching strategies for the RFIDs and this PCB basically acts as a test platform. Then, we basically miniaturize and implement the same PCB in a flexible form factor, with a co-planar waveguide designed with right characteristic impedance so as to avoid need of a matching network. Further, to implement everything end-to-end on the flexible PCB substrate, we also design a spiral antenna which fits  $1\text{ cm} \times 1\text{ cm}$  form factor (Fig. 12b). We use Ansys HFSS to optimize for the spiral dimensions (inner and outer radius), and number of turns in order to get an antenna having around 10% radiation efficiency at 900 MHz, which is similar to existing works using 900 MHz antennas in the  $1\text{ cm} \times 1\text{ cm}$  form factor [70]. Miniaturizing further is also possible but would come with slightly reduced radiation efficiencies and a reduced range. We design sensor interfacing via a similar  $1\text{ cm} \times 1\text{ cm}$  form-factor co-planar waveguide (also simulated in HFSS) with characteristic impedance matching the RFID IC. The co-planar waveguide can be miniaturized further to fit smaller antennas, but the size was kept consistent to antenna size for easier integration. Hence, the co-planar waveguide can be connected directly to the sensor+RFID IC without requiring a matching network. The co-planar waveguide and spiral antenna is implemented on a flexible PCB having polyimide substrate, which is 0.1 mm thin, and flexible enough to bend and fit various curves (Fig. 12c).

In addition to using custom designed flexible PCBs for RFID integration, ForceSticker sensor can be directly connected to commercially available printed RFID stickers (Fig. 12d). These RFID stickers have a peelable RFIC which is stuck to the two ports of the RFID antenna. We can peel the sticker with tweezers to expose the antenna pads and then interface the sensor via two tungsten filaments, one connected to each of the copper layers directly onto the antenna pads (Fig. 12d.i). Then, we can stick back the RFIC, Fig 12d.ii, such that the sensor is interfaced again in parallel to both the RFIC and antenna, without actually requiring any additional PCB.

In summary, we have three available ForceSticker platforms: the first one interfaces the sensor via a rigid  $50\text{-}\Omega$  matched PCB to an RFID IC acting as a test platform. The second approach is to interface the sensor with a flexible PCB matched directly to RFID impedance with a PCB printed antenna, which reduces the form factor to serve the in-vivo applications. The third approach interfaces the sensor in a PCB-free standalone method to existing commercial RFID stickers, to better serve the ubiquitous applications. Later in evaluations (Section 5) we show that all these three integration approaches lead to similar performance for our sensor. This shows the robustness of the two flexible form-factor integrations of ForceSticker (for in-vivo and ubiquitous applications), as they achieve errors similar to the test platform utilizing the rigid PCB+dipole antenna baseline.

#### 4.4 Reader-device Implementation

We use a Impinj Speedway R420 as the reader-device to read the ForceSticker sensor-device wirelessly. Since the channel phase measurements contain the information about force, we utilize LLURP protocol to procure phase measurements from the Speedway's FPGA via the SLLURP library in Python 3.6. The library provides almost real time phase measurements, with callback functions implemented in Python to report fresh estimates as and when provided by the LLURP messaging between the Host PC and the speedway reader. On our implementation of SLLURP [71] on a Dell Inspiron laptop with 8 GB RAM, we could get around 80-100 tag readings per second when using Impinj Hybrid Mode 1, which uses Miller 2 encoding to read RFIDs. Further, we also used the SLLURP-GUI [72] to enable real-time debugging and characterization of phase shifts for the video demo. For the reader antennas, we use the standard cross-polarized RFID antennas.

### 5 EVALUATION

In this section, we evaluate ForceSticker and present various types of experiments and case studies. We first briefly describe the experimental setups considered with the ecoflex polymer sensor having 0-6N reading range. Then we show benchmarking studies to characterize the sensor's error performance, reading the sensor even when occluded with pork belly setup and stress testing of ForceSticker with over > 10,000 force pressing events. Further, we showcase the reading ranges of about ~5m over the air in an office setting and robustness of the analog phase reading even in presence of dynamic multipath in the environment. We then show ForceSticker sensor in action for 2 case studies: sensing knee joint forces and sensing weight of contents in a package to disambiguate number of items inside it. To conclude, we show results with a different neoprene polymer sensor that can sense higher magnitude forces, to motivate how ForceSticker platform can be used with different polymer materials to tune the force sensing range as demanded by diverse applications.

#### 5.1 Experimental Setup

To benchmark ForceSticker's error performance, we build the experimental setup shown in Fig. 13. The setup consists of a linear actuator which applies forces on the sensor via an indenter. The different designed ForceSticker prototypes (all three different versions, test platform with rigid PCB and dipole antenna, flexible PCB with spiral antenna and a standalone RFID sticker) are mounted interchangeably on the load-cell platform such that the applied ground truth forces can be measured by the later, in the same way as for the wired experiments with the VNA. Until specified explicitly, we place the RFID antenna directly above the sensor at a distance of 1 m. First, we will show the results for the ecoflex sensor and 0-6N. Towards the end of the section, we show results for the neoprene sensor with force range 0-40N.

#### 5.2 Wireless Measurement Results and Sensor Benchmarking

To evaluate ForceSticker prototypes, we repeat the same experiment of applying increasing levels of forces and measuring phases as discussed in Section 4, albeit wirelessly via COTS RFID reader, instead of wired VNA measurements. First, we use the ForceSticker test platform consisting of a rigid PCB with matching network and RFID IC connected to a dipole antenna (Fig. 13 b.i). The designed rigid PCB also allows to depopulate the matching network to disconnect the sensor from the RFID IC, and then by connecting it via the UFL cable to VNA, we can obtain the ground truth phase readings from the VNA. Hence, with the test platform, in addition to wireless phase measurements, we can also collect wired phases from the VNA with the same setup which act as ground truth for error benchmarking. As seen in Fig. 14a.i, both the ground truth wired phase measurements, as well as wireless measurements across multiple experiments (three experiments shown for brevity) are consistent. This shows that the RFID reader's computed analog phases computed have good accuracy. Now to get force measurements using the computed phases, we create a sensor model using a 2nd order polynomial fit based on



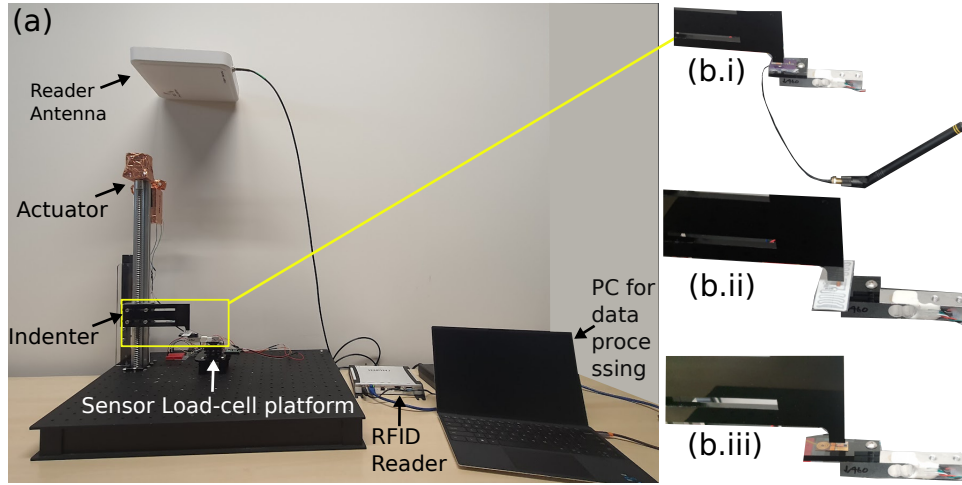


Fig. 13. (a) Experimental setup showing the sensor load cell setup, RFID reader and actuator. (b) The sensor under test can be either of the three design platforms for ForceSticker, rigid PCB+dipole antenna (b.i), standalone RFID (b.ii) and flexible PCB with spiral antenna (b.iii)

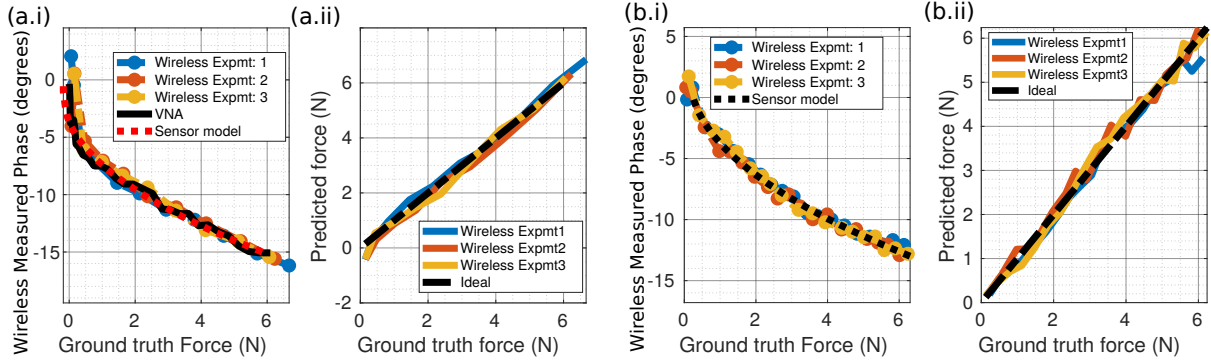


Fig. 14. (a.i) Shows the wireless measured phase changes from the ForceSticker test platform with rigid PCBs and (b.i) shows the same for standalone RFID sticker with PCB-free integration of capacitive sensor. (a.ii) and (b.ii) plots the predicted forces from the sensor model for both these sensor platforms and shows closeness to ground truth force readings, with ideal 0 error curve being when predicted and ground truth forces become equal (black dash line)

the collected VNA wired phases. This is used to compute force from phase readings, and Fig. 14a.ii shows the computed force readings from wireless phase measurements is very close to the ground truth force readings from the load cell wired force sensor.

Moving ahead, we repeat the same experiment but with the standalone RFID platform of ForceSticker (Fig. 13b.ii). A major difference here is that the sensor is fabricated with two tungsten wire filaments instead of a single one for the PCB-based integration. We observe similar results to the previous experiments (Fig. 14 b.i, b.ii), which shows the flexibility in which the designed analog sensor can be integrated to existing RFIDs, using a single tungsten wire filament on a PCB, or using two tungsten wire filaments and sticking it to the RFID antenna pads. We also repeat the same experiment with the flexible PCB platform of ForceSticker with spiral antenna (Fig. 13b.iii) to

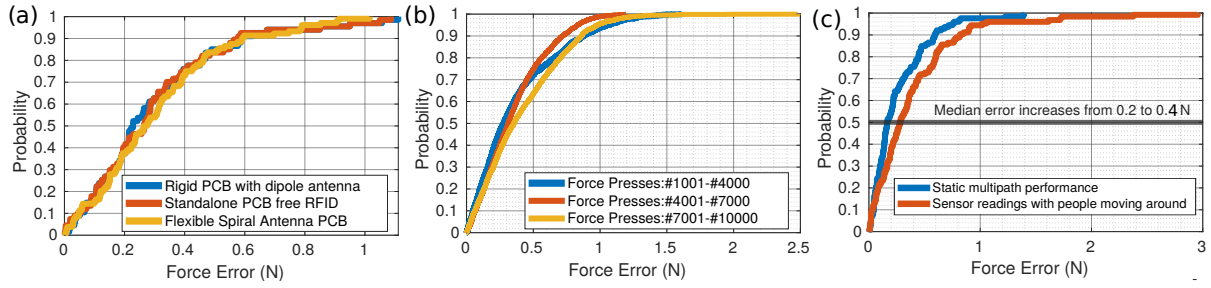


Fig. 15. Benchmark studies: (a) All the three versions of ForceSticker give similar performance (b) Pressing for multiple trials on ForceSticker doesn't create noticeable error drifts (c) Sensor error performance under multipath

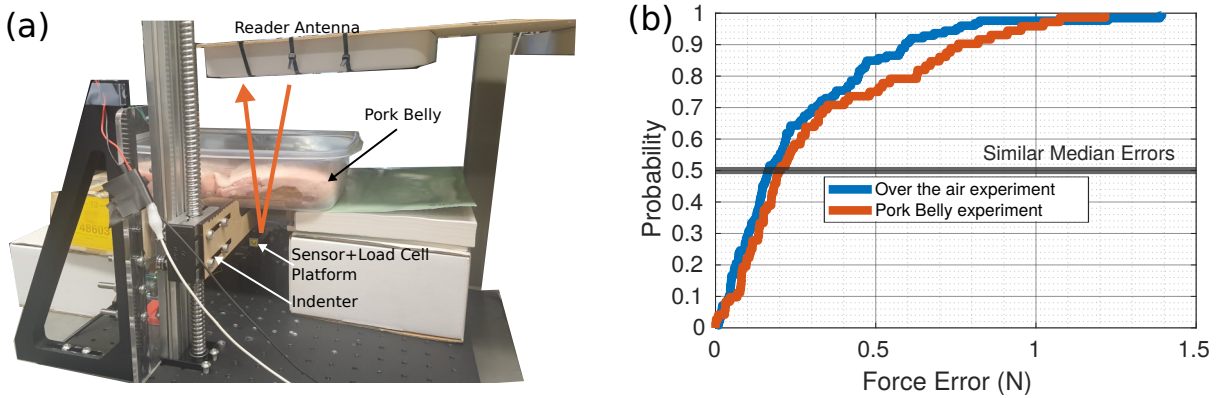


Fig. 16. (a) Shows the test setup with sensor load cell platform occluded via the pork belly, and the RFID reader antenna is placed directly over the pork belly to ensure propagation occurs via the tissues and not over the air (orange arrow) (b) Shows that having propagation over the pork belly setup doesn't adversely affect ForceSticker's sensing results

obtain similar performance (the phase to force curves are not shown for brevity sake). In order to numerically compare the error performance of all the three prototypes, we plot the force error with ground truth in form of a CDF (Fig. 15a). The CDF has these three plots more-or-less overlapping, which clearly shows that the three sensor prototypes show similar median errors of about 0.2-0.3 N. As also explained towards end of Section 3, this error stems from the channel averaged phase readings from RFID reader accurate to about  $0.5^\circ$ , and compares to reported resolution of forces felt by our fingertips as reported from HCI research [63].

We also stress test the flexible PCB platform of ForceSticker and apply more than 10,000 force presses on the sensor to see the durability of the sensor (Fig. 15b). We observe that the median error increases only slightly during the course of multiple trials on the sensor. One main reason why ForceSticker's analog capacitive sensor is durable is that it doesn't have wired interconnects. Capacitive force sensor with wired interconnects have been shown to adversely affect the durability [73]. ForceSticker's method of using minimal electronics and wireless operation doesn't suffer from these drawbacks, and hence is much more durable.

We also test ForceSticker's error performance by having 2 human volunteers walking around the sensor prototype and introducing dynamic multipath. These movements usually cause erratic phase shifts, which would adversely affect the sensor readout accuracy. We show that this can be mitigated to some extent by averaging across the multiple RFID channels. This is because different channels would see a different phase shift due to

multipath but a consistent phase shift due to applied forces (also explained towards end of Section 3). As a consequence, the median error increases slightly (from 0.2 to 0.4 N) when we have people moving around near the experimental setup (Fig. 15c). However, note that 90 percentile error increases substantially from 0.5N to  $\sim 1$ N, which shows that for 10% scenarios the erratic phase effect affects the sensor readout considerably.

Finally, we tweak our experimental setting by occluding the experimental setup with a 1200 cm<sup>2</sup> area and 10 cm thick pork belly layer (Fig. 16a), in order to verify if ForceSticker can work for in-vivo applications. The area of pork belly is  $>1000$ x the area of 1cm<sup>2</sup> sensor antenna, which ensures that the pork belly blocks the sensor completely to ensure tissue propagation paths between sensor and the RFID reader. To ensure no air signal path is present, we repeat channel measurements in anechoic chamber with and without the pork belly layer, and obtain similar additional path losses (about 10-12 dB) due to pork belly layer. These 10dB path losses from a pork belly layer (Approx 60% fat, 40% muscle) is consistent with previous reported measurements [74–76] and is not drastically high to adversely affect the sensor performance, as shown in the plotted error characterization CDF (Fig. 16b). Further, these results are consistent with past work [32, 74] which also used 900 MHz frequencies and obtained similar robust performances over the air and beneath tissues.

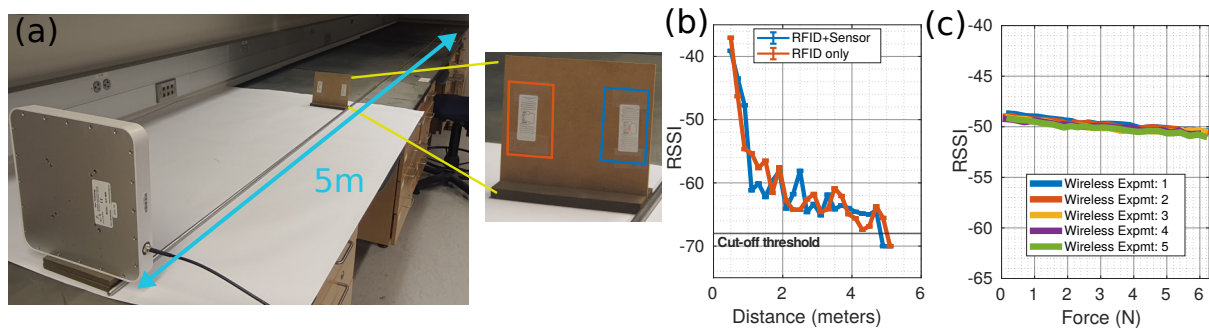


Fig. 17. (a) We move the cardboard plate away in steps of 20cm from 0.5m to 5m distance from the RFID reader antenna. The cardboard plate has two RFIDs, a vanilla RFID (orange box) and a standalone ForceSticker RFID ForceSticker (blue box) (b) Both the blue and orange RFIDs show similar RSSI drops and (c) RSSI of the RFID’s wireless channel doesn’t degrade noticeably because of applied force, unlike the channel phases. (b), (c) together show no adverse effect on the RFID wireless channel’s RSSI, and hence the reading range of both orange and blue RFIDs are similar

To conclude the sensor benchmarks, we evaluate the range of ForceSticker, and show that the integration of ForceSticker’s analog capacitive sensor into existing RFIDs does not drastically affect the reading ranges. For this experiment, we have an unaltered RFID without the sensor and a RFID integrated with the analog capacitive sensor placed close to each other and we take the signal strength readings from 0 – 5 m from the RFID reader antenna (Fig. 17a) and plot the readings side by side (Fig. 17b). We observe that the RFID with sensor fails to be read beyond 4.6 m, whereas the standard RFID goes till 4.8 m, which is only minimally more than capacitive sensor + RFID. The reason for this is the fact that the sensor is purely capacitive and mostly produces change in signal phase when force is applied, and does not change the signal amplitude by much. This is also shown when we plot the RSSI vs force for the sensor, placed at about 1 m away, and see that unlike phase readings which show changes as force is applied, the RSSI readings stay more or less constant (Fig. 17c), with only a dip of about  $-1$  dB (and hence the minimal range reduction of 0.2 m). Although 5m is a reasonable range of operation, this can be further improved by higher quality tags [77], or by using multi-antenna readers capable of beamforming towards the tag [78].

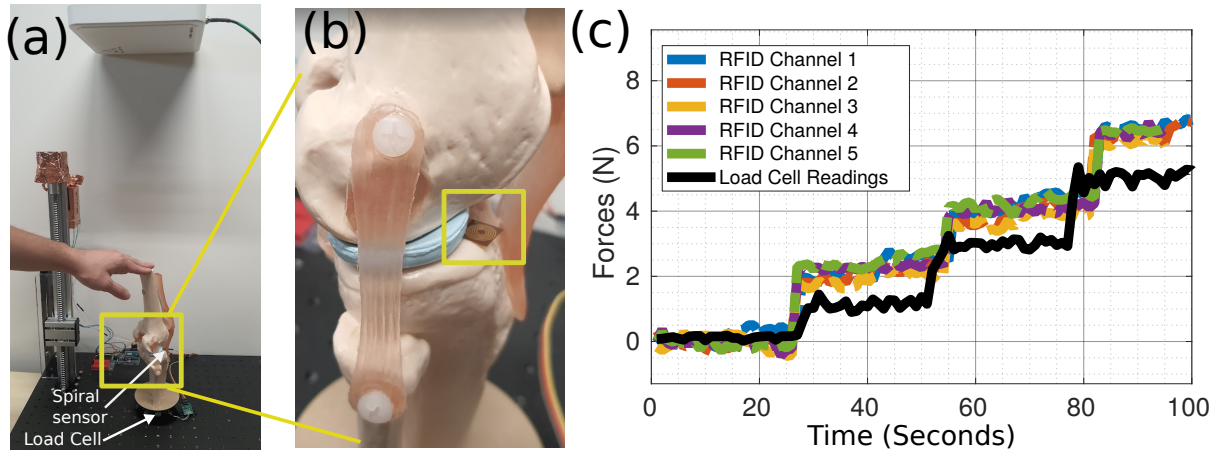


Fig. 18. (a) Test Setup, (b) Zoomed image to show the flexible PCB ForceSticker snugly fit within the knee-joint, (c) ForceSticker’s wireless force readings correlates well with the force readings from the load cell placed below the knee

### 5.3 Case Study 1: Knee Force Measurement

For the first case study, we place the flexible PCB ForceSticker platform with spiral antenna beneath the knee joint (Fig. 18a,b) in a toy-knee model and apply forces onto the sensor by pressing on the top of the knee bone manually. As seen clearly the small size form factor of ForceSticker sensor fits inside the knee joint without disturbing the joint at all and is almost un-noticeable if viewed from a distance. To see if the sensor is able to detect the applied forces, we apply roughly 1 N, 3 N, 5 N force in steps delayed by 20 sec via a human operator (also shown in supplemental video). This is made possible by showing the applied forces on to the human operator, who can then manually adjust the applied force to meet the 1, 3, 5 N target. The load cell is compensated to zero at the knee-model’s weight to compensate for the static gravitational force. Because of this compensation, the actual applied forces on the sensor is the applied force by hand + static weight of the top part of the knee model relatively to the joint (approximately 1 N) and hence the readings reported by the sensor are 1 N offsetted when the sensor is manually pressed. The phases collected (and hence the estimated forces) show repeatable behaviour across the various channels and show three clean jumps corresponding to when the sensor is pressed with higher forces (Fig. 18c), which shows that the sensor was indeed able to capture the applied forces via the knee joints. This motivates the use of ForceSticker sensors to create smart implants, which can sense the applied forces and can be then used to monitor the implant health.

One point to note here is that via the toy-knee model we can get forces in range of 0-6 N, however in an actual knee the forces would be much higher (say for a person weighing 60 Kg, the force on the joint could be as high as 300 N). So, in actual use-case the sensor has to be re-designed for higher forces and we present simulation results with a stiffer variant of the neoprene polymer (carbon filled neoprene rubber) capable of sensing till 600N. Note that performing an actual knee-joint sensing experiment is out of scope for this paper and requires IRB clearances in addition, and hence hardware verification of the carbon-black neoprene sensor constitutes our future work. However, this case study still showcases two key results, one, the sensor can fit into these tight constraint spaces and two, the sensor can read forces applied unevenly by the joints in addition to the previous results shown when sensor was pressed by an actuated indenter.

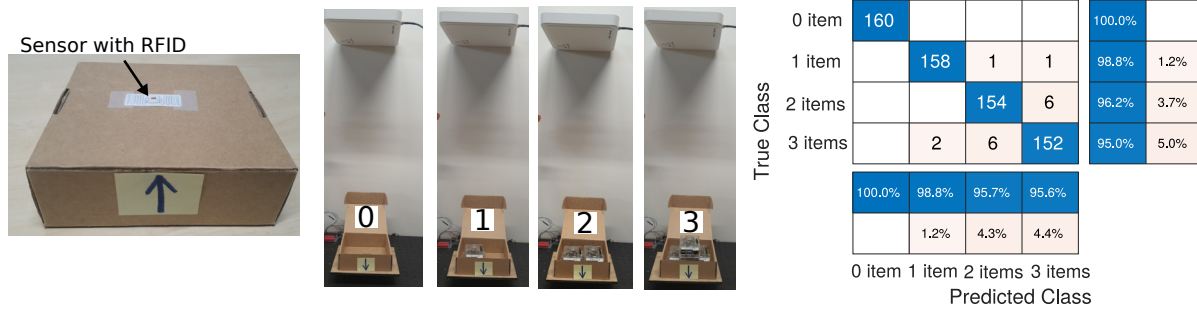


Fig. 19. Weighing objects placed in a box with ForceSticker RFID sticker stuck to the bottom of the package: By measuring the weight of the contents, ForceSticker is able to classify the number of contents in the box

#### 5.4 Case Study 2: Box Item Weighing

Now, for the second case study, we stick the PCB-free standalone RFID sticker platform of ForceSticker to the bottom of a cardboard package. We show the basic principle of how the sensor can be used to sense applied weight on it in the supplemental video. For the case study, we place 3 items in the box one at a time, and record the phase shifts from the sensor (Fig. 19). For the experiment, we choose the item as a Raspberry Pi 4 with a plastic case which weighs about 200 g and hence applies 2 N force on the sensor. Hence, when 1 item is placed the sensor would be under 2 N force, which then increases to 4 N and finally 6 N when three items are placed. The reader is able to identify the number of items placed in the box since when more items are kept in the box, more gravitational force is applied to the sensor and hence there is a different associated phase shift when the items are placed. We take 160 measurements of placing items in the box and classify the number of items based on the measured phase difference (and hence the force), to plot the confusion matrix as shown in Fig. 19. The sensor is able to detect the classes with > 95% accuracy, with the higher forces being slightly confused with lower ones, because the force to phase profile is not exactly linear and the phase difference between 4 N and 6 N is lesser than the difference between 0 N, 2 N and 2 N, 4 N. However, since even the 95% errors of ForceSticker as seen from CDFs before are about 1 N, these results are consistent with the CDF profiling of force readings. Hence, this case-study motivates the usecase of ForceSticker in warehouse settings (for example say amazon warehouses) where the sensor readings can be used to determine the number of items inside the package wirelessly by just reading the RFIDs and perform easy integrity checks via the same.

#### 5.5 Generalization to Higher Force Range of 40N

So far, we have presented results with ecoflex as the soft polymer dielectric in the capacitive sensor. One problem with ecoflex is that in our experiments we observed it to break at 7N mark, and hence our force range was limited to 0-6N. However, in order to sense higher magnitude force, we can choose a sturdier and more rigid polymer, for example neoprene. We design similar geometry sensor with Neoprene 30A layer (4mm\*2mm) but thicker polymer height (2mm instead of 0.2mm) to account for higher dielectric of neoprene and increased stiffness. The neoprene sensor designed provides similar  $20^\circ$  phase change albeit over higher force range 0-40N (Fig. 20). As a consequence of similar force range, the expected error would scale linearly as well, since the force range is agnostic to RFID reader and it would just use a different scaled sensor model. Since the measured error with ecoflex sensor is  $\sim 0.25N$  for 0-6N range, the expected error for 0-40N sensor would be  $0.25 * \frac{40}{6} = 1.7N$ , which is close to what we obtain experimentally. This result shows how ForceSticker can use different polymers



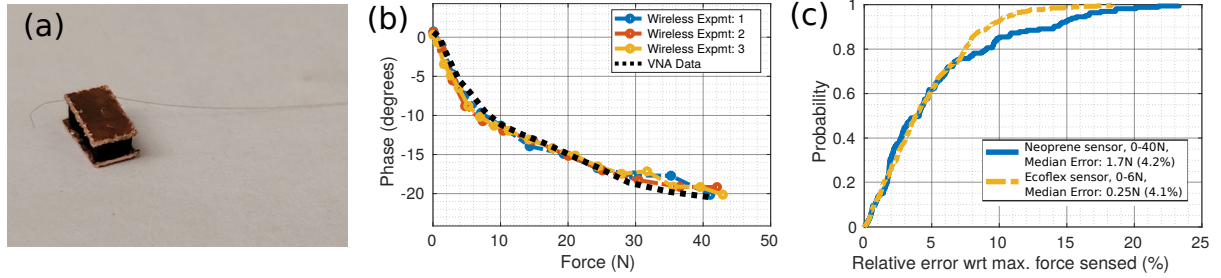


Fig. 20. (a) Shows the neoprene polymer capacitive sensor, capable of sensing forces upto 40N, with (b) Showing about  $20^\circ$  phase change as the applied force reaches 40N and (c) Shows the CDF of relative error wrt maximum sensed force for both neoprene and ecoflex sensor. Since the overall phase change is similar but for different force ranges, both the sensors show similar median CDF performance of 5% relative error

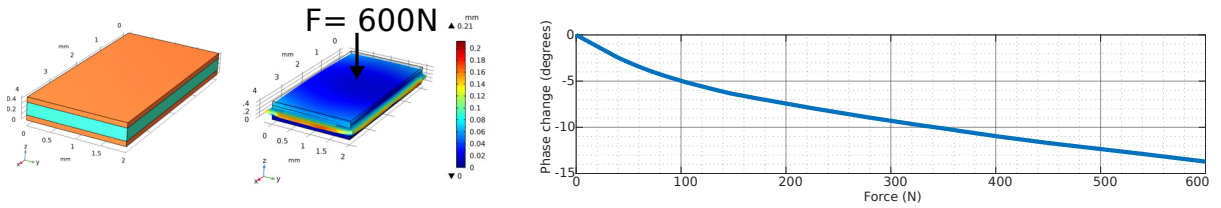


Fig. 21. Simulations depicting carbon black neoprene sensor, that creates  $15^\circ$  phase changes with 600N applied forces

to adapt to different force ranges. Further, the error characterization shows the dependence of error on the phase changes, which would scale linearly if the phase changes are targeted to be similar over a different force range.

## 6 DISCUSSION AND LIMITATIONS

### 6.1 Scaling the Sensor to 0-600N Forces for Orthopaedic Implant Application

ForceSticker utilizes two different analog capacitive sensors: first, a ecoflex force sensor (shore hardness 0030) which works for 0 – 6 N range, and second, neoprene rubber (shore hardness 30A) sensor which works for 0 – 40 N range. Basically, neoprene is a stiffer polymer with higher shore hardness, which allows sensing of higher magnitude forces. Now, we can choose an even stiffer version of neoprene rubber, which is carbon black filled neoprene rubber, which allows sensing of even higher magnitude forces (0-600N), which can better motivate the orthopaedic force-sensor backed implant application of ForceSticker. However, we can not test the carbon black filled capacitive sensor with our existing test setup of load cells and actuators, which is limited to 50N and hence fabricating and testing a 0-600N sensor is outside the scope of this paper. However, to present that the capacitive sensor can scale up to 0-600N, we present simulation results with 0.45 mm thick carbon filled neoprene polymer [79], layer. This sensor designs give similar phase change results (about  $15^\circ$ ) for both the higher (0 – 600) N force ranges (Fig. 21), and hence the wireless error performance will be similar to the prototyped sensors in the paper. As shown in Fig. 20(c), the sensors have median errors < 5% of the maximum force sensing range. For the carbon-black neoprene sensor, with maximum force of 600N, 5% calculates to 30N and this error of 30N is acceptable norm for the orthopaedic knee application. Similar error metrics of  $\sim 30$ N are presented via case-studies with wired force-sensors to motivate force-sensor backed orthopaedic implants [44].

## 6.2 Reading Forces from Multiple Sensors Concurrently

In ForceSticker evaluations, we have used the commercial RFID reader to read from one force-sensor interfaced RFID at a time. However, RFID MAC utilizing the popular EPC Gen 2 protocol has advanced significantly over the years. The RFID MAC easily generalises to multiple tag readings via the same RFID reader, and then by observing the channel estimates we can estimate the applied forces on each of the tag. Thus, ForceSticker sensing principle extends very naturally to multiple such force sensors. Hence, ForceSticker can easily demonstrate this capability to read from multiple tags concurrently and motivate new applications where reading from large number of tags simultaneously would be beneficial.

## 6.3 Integration with Other Backscatter Technologies

ForceSticker shows how we can design such analog backscatter sensors and integrate them to existing RFID ICs which provide digital identity to the sensor. This feature of ForceSticker's analog capacitive sensor requiring a simple digital identity also allows possible integration with upcoming backscatter technologies as well, like Wi-Fi [40, 41], LoRA[80, 81], UWB backscatter[82], or a multi-platform detectable frequency shift [24, 32]. Unlike UHF RFID as used in this paper, these other backscatter technologies are still under research with no commercially available IC to interface the sensor in the present day. But, in the future, such analog capacitive force sensors can be integrated with the new technologies to provide digital identities readable via different wireless protocols.

## 6.4 Bio-compatible Hermetic Packaging of the Sensor

Although we fabricate ForceSticker on flexible sticker-like RFIDs and PCBs, and also show them working beneath the pork belly and embedded inside the toy-knee model, another important step is to cover the whole sensor in a bio-compatible packing which is also known as hermetic packing, which refers to airtight moisture-tight packing. This would also allow testing the sensor when it is embedded inside pork-belly instead of placing it below the pork belly. There have been previous examples of hermetically packed batteryless sensors used in-vivo, for example wireless monitoring of blood pressure near the arteries [83, 84] and non-invasive EMG recording [85] which use materials like nitinol and medical grade epoxy to encapsulate the sensor and pack it hermetically. In the future, ForceSticker can also adopt similar methods and encapsulate the sensor-sticker to make it bio-compatible.

## 6.5 Force Sensing with Sensor Under Movement

In ForceSticker evaluations the sensor is kept fixed and not moved when forces are applied onto it. However, for applications like safe control of robot via force feedback, or fast moving orthopaedic implant force sensing, the attached sensor to these usecases will not be stationary. Although we have shown that ForceSticker's sensing strategy is robust to movement of environmental entities after averaging across the RFID channels, when the sensor itself starts to move simple averaging won't help to compensate for movement induced phase changes. These mechanical movements would show up with a periodic time signature, or with a certain spectral signature, which can be isolated by taking a frequency transform of the phase readings as shown by past RFID sensing and localization works [52]. Hence, in the future, we can also write a frequency transform to remove the movement artefacts and make the ForceSticker sensors robust to sensor movements.

## 6.6 Limitations in Reading Package Weight from ForceSticker

For our case study in Section 5.4, we assume that ForceSticker is stuck at the center and aligned such that it faces the bottom of the package such that the entire average weight of package acts onto it. This is similar to the weight sensing demo shown in the supplementary video. However, this may not be the case in real scenario, where the weight may be distributed across the package. One way to handle this is to keep multiple stickers across the package bottom. and that would capture a weight profile which can help determine the total weight of

the package. Since ForceSticker is a simple RFID tag which costs <1\$ per tag it is possible to have ~3 – 4 such tags stuck to ensure sensing of the entire weight profile.

## 7 RELATED WORKS

ForceSticker presents the first batteryless sticker-like form factor force sensors which enable diverse set of applications ranging from ubiquitous weight sensing to in-vivo applications. In this section we will compare the past work on force sensors and RFID based sensing and put them in context with ForceSticker's contributions.

### 7.1 Discrete MEMS Force Sensors

Force sensors has been an active area of research over the past years in the flexible electronics and MEMS sensor communities [9, 16, 86–93]. Today's force sensors can be roughly divided into three groups, impedance based sensors, piezo sensors and magnetic sensors [10–12, 14, 15, 17, 73, 94–96]. The impedance based sensors usually transduce force onto changes in sensor resistance [9–11] or capacitance [12, 13, 97]. The piezo sensors generate small voltages as a function of contact forces applied onto the sensor [15, 17, 94, 98]. The magnetic sensors create distortions in magnetic field due to the applied force [73, 96, 99, 100]. A unifying theme of these three sensor types is the fact that they all need to be digitized before communicating these readings to remotely located wireless reader. This is because the effect generated by force can not be read directly at a considerable distance, as ultimately these sensors map to either voltage or magnetic field fluctuations which die out within few centimeters. Typically, past work addresses this by using amplifiers and digitization blocks in Data acquisition units (DAQs) for the sensors. Usually, a DAQ would consist of OPAMP amplifier circuits, ADCs for resistive and piezo sensors [34, 35], CDCs for capacitive sensors [13, 36], and magnetometers for magnetic sensors [73, 99]. After digitization, the values are modulated onto a wireless signal to communicate the readings to a distance. However, this process of digitization, and further modulation usually requires dedicated electronics typically in form of low-power embedded microcontrollers which do not allow these MEMS sensors to attain the batteryless and sticker like form factor for wireless force feedback.

### 7.2 Joint Communication and Sensing Based Force Sensors

ForceSticker sensor shows how force can be transduced to wireless signal phases directly, without requiring these extra digitization+modulation steps. Thus, the sensors which enable a similar wireless transduction form the closest related works to ForceSticker, however none of them can be read as robustly, nor have the sticker-like form factor like ForceSticker. A common set of works utilize inductor coils with capacitive sensors to form LC circuits [101–104]. LC circuits have the property of absorbing a certain resonant frequency depending on the value of capacitance, and thus as the force applied changes capacitance, the force information gets transduced onto the resonant frequency absorbed. However, these sensors have shown limited range (few cm), and unreliable reading in cluttered environments, and less dynamic range as the resonant frequency shifts only by a few kHz/MHz [102, 105]. Further, these sensors do not generalize easily to multiple sensors since there is no way to determine the identity of certain sensor from the resonant frequency alone.

Similar to LC sensors, we have strain sensors which can be SAW based [106–109], or even some RFID based strain sensors [110]. These strain sensors don't really sense the contact force but are capable of sensing the shear forces which create elongations. These elongations change the physical dimensions of the RFID antenna, or the SAW channel filter, which again leads to changes in the antenna's resonant frequency and thus can be sensed similar to LC sensors, and have similar drawbacks on not generalizing to a variety of environments since other objects in environment also absorb certain frequencies [107]. Another prior work [32, 111] also attempts to map force to phase, however as discussed earlier does not achieve the sticker form factor and the designed prototype is not batteryless since it is not evaluated with an energy harvester.

### 7.3 RFID Based sensing of Temperature, Light, Touch Gestures and Other Quantities

In addition to design of a mm-scale force sensor, we have also shown how to integrate the sensor with RFID systems. There has been a vast body of works on how to use RFIDs to sense effects like environmental temperature [53, 112], moisture [113, 114], photointensity [31, 115], binary touch/no-touch [52, 116, 117] etc. One particular past work showcases a generalized framework for interfacing various sensors with RFIDs [31], however this method ends up compromising the RFID read range since the main method of sensing proposed is differential wake up thresholds. This ends up hampering the sensor resolution as well since the amplitude of reflected signals decreases. Also [31] just motivates the possibility of force (pressure) sensor integration with the proposed system, but does not explicitly evaluate it like how temperature and photointensity were evaluated. In ForceSticker we show how to integrate force sensors without affecting the range of the RFID, by doing a purely phase based transduction, and even integrating with common commercially available RFID tags.

Unlike the other sensed quantities, force sensing has not been extensively studied for RFID sensing systems. There has been just a single work [38] which used a particular SL900A RFID tag [39] that exposes an ADC interface to allow connecting various sensors, and the authors of [38] connect up a force sensitive resistor to the ADC pin. However, this interfacing of the resistor to the ADC pin requires extra accompanying electronics to enable sensor data buffering and data register writing which put a massive burden on energy harvester since RFIDs operate on a very tight energy budget. In comparison, ForceSticker allows for force sensors to be integrated in analog domain with RFIDs without putting extra burden on the digital communication, and allowing for integration with any commercially available tag today, not just a specialized tag with ADC pins.

Finger touch sensing is another popular application of RFID sensing systems [52, 117–123], which is related to force sensing however usually these systems sense gestures and binary contact/no-contact. IDSense [123], PaperId [52] and RIO [117] are some notable works which demonstrate relationship between phases and finger touches, simple manufacturing of such touch sensitive tags as well as multi-RFID touch generalization. However, these past works are oblivious to different force levels applied during the touch process, and these works just sense the places where the tag is interrogated via the fingers to sense simple gestures/sliding movements etc.

## REFERENCES

- [1] Eric H Ledet, Benjamin Liddle, Katerina Kradinova, and Sara Harper. Smart implants in orthopedic surgery, improving patient outcomes: a review. *Innovation and entrepreneurship in health*, 5:41, 2018.
- [2] Boyd M Evans, Mohamed R Mahfouz, and Emily R Pritchard. Biocompatible mems electrode array for determination of three-dimensional strain. In *2006 International Conference of the IEEE Engineering in Medicine and Biology Society*, pages 4092–4095. IEEE, 2006.
- [3] C Blanes, V Cortés, C Ortiz, M Mellado, and P Talens. Non-destructive assessment of mango firmness and ripeness using a robotic gripper. *Food and bioprocess technology*, 8(9):1914–1924, 2015.
- [4] S Fatikow et al. Micro-force sensing in a micro-robotic system. In *Proceedings 2001 ICRA. IEEE International Conference on Robotics and Automation (Cat. No. 01CH37164)*, volume 4, pages 3435–3440. IEEE, 2001.
- [5] AH Hosseinabadi and Septimiu E Salcudean. Force sensing in robot-assisted keyhole endoscopy: A systematic survey. *arXiv preprint arXiv:2103.11123*, 2021.
- [6] Hedan Bai, Shuo Li, Jose Barreiros, Yaqi Tu, Clifford R Pollock, and Robert F Shepherd. Stretchable distributed fiber-optic sensors. *Science*, 370(6518):848–852, 2020.
- [7] Minglu Zhu, Zhongda Sun, Zixuan Zhang, Qiongfeng Shi, Tianyiyi He, Huicong Liu, Tao Chen, and Chengkuo Lee. Haptic-feedback smart glove as a creative human-machine interface (hmi) for virtual/augmented reality applications. *Science Advances*, 6(19):eaaz8693, 2020.
- [8] Wang Dangxiao, Guo Yuan, Liu Shiyi, Yuru Zhang, Xu Weiliang, and Xiao Jing. Haptic display for virtual reality: progress and challenges. *Virtual Reality & Intelligent Hardware*, 1(2):136–162, 2019.
- [9] Ilya Rosenberg and Ken Perlin. The unmousepad: an interpolating multi-touch force-sensing input pad. In *ACM SIGGRAPH 2009 papers*, pages 1–9. 2009.
- [10] X Zhang, AK Bose, D Maddipatla, S Masih, V Palaniappan, M Panahi, BB Narakathu, and MZ Atashbar. Development of a novel and flexible mwcnt/pdms based resistive force sensor. In *2020 IEEE International Conference on Flexible and Printable Sensors and Systems*

- (FLEPS), pages 1–4. IEEE, 2020.
- [11] Giovanni Saggio, Francesco Riillo, Laura Sbernini, and Lucia Rita Quitadamo. Resistive flex sensors: a survey. *Smart Materials and Structures*, 25(1):013001, 2015.
  - [12] Kyoung-Ho Ha, Heeyong Huh, Zhengjie Li, and Nanshu Lu. Soft capacitive pressure sensors: Trends, challenges, and perspectives. *ACS nano*, 16(3):3442–3448, 2022.
  - [13] Moran Amit, Rupesh K Mishra, Quyen Hoang, Aida Martin Galan, Joseph Wang, and Tse Nga Ng. Point-of-use robotic sensors for simultaneous pressure detection and chemical analysis. *Materials Horizons*, 6(3):604–611, 2019.
  - [14] Ahmed Salim and Sungjoon Lim. Review of recent inkjet-printed capacitive tactile sensors. *Sensors*, 17(11):2593, 2017.
  - [15] Patricia W Freeman and Cliff A Lemen. Measuring bite force in small mammals with a piezo-resistive sensor. *Journal of Mammalogy*, 89(2):513–517, 2008.
  - [16] Yuzhang Wei and Qingsong Xu. An overview of micro-force sensing techniques. *Sensors and Actuators A: Physical*, 234:359–374, 2015.
  - [17] William Navaraj and Ravinder Dahiya. Fingerprint-enhanced capacitive-piezoelectric flexible sensing skin to discriminate static and dynamic tactile stimuli. *Advanced Intelligent Systems*, 1(7):1900051, 2019.
  - [18] IF Cengiz, M Pitikakis, L Cesario, P Parascandolo, L Vosilla, G Viano, JM Oliveira, and RL Reis. Building the basis for patient-specific meniscal scaffolds: from human knee mri to fabrication of 3d printed scaffolds. *Bioprinting*, 1:1–10, 2016.
  - [19] Santiago Restrepo, Eric B Smith, and William James Hozack. Excellent mid-term follow-up for a new 3d-printed cementless total knee arthroplasty. *The Bone & Joint Journal*, 103(6 Supple A):32–37, 2021.
  - [20] S Sporer, L MacLean, A Burger, and M Moric. Evaluation of a 3d-printed total knee arthroplasty using radiostereometric analysis: assessment of highly porous biological fixation of the tibial baseplate and metal-backed patellar component. *The bone & joint journal*, 101(7\_Supple\_C):40–47, 2019.
  - [21] Mohamed R Abdelhamid, U Ha, Utsav Banerjee, Fadel Adib, and A Chandrakasan. Wireless, batteryless, and secure implantable system-on-a-chip for 1.37 mmhg strain sensing with bandwidth reconfigurability for cross-tissue adaptation. In *2022 IEEE Custom Integrated Circuits Conference (CICC)*, pages 1–2. IEEE, 2022.
  - [22] Po-Han Peter Wang, Chi Zhang, Hongsen Yang, Manideep Dunna, Dinesh Bharadia, and Patrick P Mercier. A low-power backscatter modulation system communicating across tens of meters with standards-compliant wi-fi transceivers. *IEEE Journal of Solid-State Circuits*, 55(11):2959–2969, 2020.
  - [23] Vincent W Leung, Jihun Lee, Siwei Li, Siyuan Yu, Chester Kilfove, Lawrence Larson, Arto Nurmikko, and Farah Laiwalla. A cmos distributed sensor system for high-density wireless neural implants for brain-machine interfaces. In *ESSCIRC 2018-IEEE 44th European Solid State Circuits Conference (ESSCIRC)*, pages 230–233. IEEE, 2018.
  - [24] Vaishnavi Ranganathan, Sidhant Gupta, Jonathan Lester, Joshua R Smith, and Desney Tan. Rf bandaid: A fully-analog and passive wireless interface for wearable sensors. *Proceedings of the ACM on Interactive, Mobile, Wearable and Ubiquitous Technologies*, 2(2):1–21, 2018.
  - [25] Mohamed R Abdelhamid, Ruicong Chen, Joonhyuk Cho, Anantha P Chandrakasan, and Fadel Adib. Self-reconfigurable micro-implants for cross-tissue wireless and batteryless connectivity. In *MobiCom'20: Proceedings of the 26th Annual International Conference on Mobile Computing and Networking*, 2020.
  - [26] Jihun Lee, Ethan Mok, Jiannan Huang, Lingxiao Cui, Ah-Hyoung Lee, Vincent Leung, Patrick Mercier, Steven Shellhammer, Lawrence Larson, Peter Asbeck, et al. An implantable wireless network of distributed microscale sensors for neural applications. In *2019 9th International IEEE/EMBS Conference on Neural Engineering (NER)*, pages 871–874. IEEE, 2019.
  - [27] Devdip Sen, John McNeill, Yitzhak Mendelson, Raymond Dunn, and Kelli Hickie. Wireless sensor patch suitable for continuous monitoring of contact pressure in a clinical setting. In *2018 16th IEEE International New Circuits and Systems Conference (NEWCAS)*, pages 91–95. IEEE, 2018.
  - [28] John McNeill, Devdip Sen, Yitzhak Mendelson, Matthew Crivello, Shamsur Mazumder, Amanda Agdeppa, Syed Ali Hussein, Hyunsoo Kim, Victoria Loehle, Raymond Dunn, et al. Wearable wireless sensor patch for continuous monitoring of skin temperature, pressure, and relative humidity. In *2017 IEEE International Symposium on Circuits and Systems (ISCAS)*, pages 1–4. IEEE, 2017.
  - [29] CM Yang, TL Yang, CC Wu, SH Hung, MH Liao, MJ Su, and HC Hsieh. Textile-based capacitive sensor for a wireless wearable breath monitoring system. In *2014 IEEE International Conference on Consumer Electronics (ICCE)*, pages 232–233. IEEE, 2014.
  - [30] Talha Agcayazi, Michael McKnight, Peter Sotory, Helen Huang, Tushar Ghosh, and Alper Bozkurt. A scalable shear and normal force sensor for prosthetic sensing. In *2017 IEEE SENSORS*, pages 1–3. IEEE, 2017.
  - [31] Ju Wang, Omid Abari, and Srinivasan Keshav. Challenge: Rfid hacking for fun and profit. In *Proceedings of the 24th Annual International Conference on Mobile Computing and Networking*, pages 461–470, 2018.
  - [32] Agrim Gupta, Cédric Girerd, Manideep Dunna, Qiming Zhang, Raghav Subbaraman, Tania Morimoto, and Dinesh Bharadia. {WiForce}: Wireless sensing and localization of contact forces on a space continuum. In *18th USENIX Symposium on Networked Systems Design and Implementation (NSDI 21)*, pages 827–844, 2021.
  - [33] Sensel. Sensel force sensitive trackpads. <https://sensel.com/>, 2022.



- [34] Ravinder S Dahiya, Davide Cattin, Andrea Adami, Cristian Collini, Leonardo Barboni, Maurizio Valle, Leandro Lorenzelli, Roberto Oboe, Giorgio Metta, and Francesca Brunetti. Towards tactile sensing system on chip for robotic applications. *IEEE Sensors Journal*, 11(12):3216–3226, 2011.
- [35] Ali Ibrahim, Luigi Pinna, and Maurizio Valle. Experimental characterization of dedicated front-end electronics for piezoelectric tactile sensing arrays. *Integration*, 63:266–272, 2018.
- [36] Uikyum Kim, Dong-Hyuk Lee, Woon Jong Yoon, Blake Hannaford, and Hyouk Ryeol Choi. Force sensor integrated surgical forceps for minimally invasive robotic surgery. *IEEE Transactions on Robotics*, 31(5):1214–1224, 2015.
- [37] Hi-Tech Glitz. The airpods pro’s force sensor is a more convenient way to control audio. <https://hitechglitz.com/the-airpods-pros-force-sensor-is-a-more-convenient-way-to-control-audio/>, 2022.
- [38] José Fernández-Salmerón, Almudena Rivadeneyra, Fernando Martínez-Martí, Luis Fermín Capitán-Vallvey, Alberto J Palma, and Miguel A Carvajal. Passive uhf rfid tag with multiple sensing capabilities. *Sensors*, 15(10):26769–26782, 2015.
- [39] AMS. Ams sl900a. <https://ams.com/en/sl900a>, 2022.
- [40] Pengyu Zhang, Dinesh Bharadia, Kiran Joshi, and Sachin Katti. Hitchhike: Practical backscatter using commodity wifi. In *Proceedings of the 14th ACM Conference on Embedded Network Sensor Systems CD-ROM*, SenSys ’16, page 259–271, New York, NY, USA, 2016. Association for Computing Machinery.
- [41] Pengyu Zhang, Colleen Josephson, Dinesh Bharadia, and Sachin Katti. Freerider: Backscatter communication using commodity radios. In *Proceedings of the 13th International Conference on Emerging Networking EXperiments and Technologies*, CoNEXT ’17, page 389–401, New York, NY, USA, 2017. Association for Computing Machinery.
- [42] Zicheng Chi, Xin Liu, Wei Wang, Yao Yao, and Ting Zhu. Leveraging ambient lte traffic for ubiquitous passive communication. In *Proceedings of the Annual conference of the ACM Special Interest Group on Data Communication on the applications, technologies, architectures, and protocols for computer communication*, pages 172–185, 2020.
- [43] Mohsen Safaei, R Michael Meneghini, and Steven R Anton. Force detection, center of pressure tracking, and energy harvesting from a piezoelectric knee implant. *Smart materials and Structures*, 27(11):114007, 2018.
- [44] David Forchelet, Matteo Simoncini, Arash Arami, Arnaud Bertsch, Eric Meurville, Kamiar Aminian, Peter Ryser, and Philippe Renaud. Enclosed electronic system for force measurements in knee implants. *Sensors*, 14(8):15009–15021, 2014.
- [45] Dimitrios Kosmas, Hans-Peter van Jonbergen, Martijn Schouten, Momen Abayazid, and Gijs Krijnen. Development of a 3d printed gap gauge with embedded force sensor for balancing unicompartmental knee arthroplasty. In *2021 IEEE Sensors*, pages 1–4, 2021.
- [46] Michael Yip and David Camarillo. Model-less hybrid position/force control: a minimalist approach for continuum manipulators in unknown, constrained environments. *IEEE Robotics and Automation Letters*, 2016.
- [47] Aude Billard and Danica Kragic. Trends and challenges in robot manipulation. *Science*, 364(6446), 2019.
- [48] Zhen Deng, Yannick Jonetzko, Liwei Zhang, and Jianwei Zhang. Grasping force control of multi-fingered robotic hands through tactile sensing for object stabilization. *Sensors*, 20(4):1050, 2020.
- [49] Josiah Hester and Jacob Sorber. The future of sensing is batteryless, intermittent, and awesome. In *Proceedings of the 15th ACM conference on embedded network sensor systems*, pages 1–6, 2017.
- [50] Akshay Gadre, Deepak Vasisht, Nikunj Raghuvanshi, Bodhi Priyantha, Manikanta Kotaru, Swarun Kumar, and Ranveer Chandra. Milton: Sensing product integrity without opening the box using non-invasive acoustic vibrometry. In *2022 21st ACM/IEEE International Conference on Information Processing in Sensor Networks (IPSN)*, pages 390–402. IEEE, 2022.
- [51] Eleonora Bottani, Martina Mantovani, Roberto Montanari, and Giuseppe Vignali. Inventory management in the presence of inventory inaccuracies: an economic analysis by discrete-event simulation. *International Journal of Supply Chain and Inventory Management*, 2(1):39–73, 2017.
- [52] Hanchuan Li, Eric Brockmeyer, Elizabeth J Carter, Josh Fromm, Scott E Hudson, Shwetak N Patel, and Alanson Sample. Paperid: A technique for drawing functional battery-free wireless interfaces on paper. In *Proceedings of the 2016 CHI Conference on Human Factors in Computing Systems*, pages 5885–5896, 2016.
- [53] Swadhin Pradhan and Lili Qiu. Rtsense: passive rfid based temperature sensing. In *Proceedings of the 18th Conference on Embedded Networked Sensor Systems*, pages 42–55, 2020.
- [54] Rene Hartansky, Martin Mierka, Vladimir Jancarik, Mikulas Bittera, Jan Halgos, Michal Dzuris, Jakub Krchnak, Jaroslav Hricko, and Robert Andok. Towards a mems force sensor via the electromagnetic principle. *Sensors*, 23(3):1241, 2023.
- [55] Agrim Gupta, Cédric Girerd, Manideep Dunna, Qiming Zhang, Raghav Subbaraman, Tania Morimoto, and Dinesh Bharadia. Expanding the horizons of wireless sensing: Sensing and localizing contact forces with signal reflections. *GetMobile: Mobile Computing and Communications*, 25(3):38–42, 2022.
- [56] Seunghyun Eom and Sungjoon Lim. Stretchable complementary split ring resonator (csrr)-based radio frequency (rf) sensor for strain direction and level detection. *Sensors*, 16(10):1667, 2016.
- [57] Comsol. Comsol multiphysics 6.0. <https://www.comsol.com/release/6.0>, 2022.
- [58] Frederic Thiesse and Florian Michahelles. An overview of epc technology. *Sensor review*, 2006.

- [59] Skyworks Application Note. Smv1245-011. <https://www.skyworksinc.com/-/media/CDB4D839CD584C54ADF09007F91D37B2.pdf>, 2022.
- [60] Chien-San Lin, Sheng-Fuh Chang, and Wen-Chun Hsiao. A full-360-degree reflection-type phase shifter with constant insertion loss. *IEEE Microwave and Wireless Components Letters*, 18(2):106–108, 2008.
- [61] Teng Wei and Xinyu Zhang. Gyro in the air: tracking 3d orientation of batteryless internet-of-things. In *Proceedings of the 22nd Annual International Conference on Mobile Computing and Networking*, pages 55–68, 2016.
- [62] GS1 Low Level Reader Protocol (LLRP) Standard. Llrp. [https://www.gs1.org/docs/epc/LLRP\\_standard\\_i2\\_r\\_2021-01-27.pdf](https://www.gs1.org/docs/epc/LLRP_standard_i2_r_2021-01-27.pdf), 2022.
- [63] Axel Antoine, Sylvain Malacria, and Géry Casiez. Forceedge: controlling autoscroll on both desktop and mobile computers using the force. In *Proceedings of the 2017 CHI Conference on Human Factors in Computing Systems*, pages 3281–3292, 2017.
- [64] Faika F Hanna, Kamal N Abdel-Nour, and Salwa L Abdel-Messieh. Dielectric properties of some synthetic rubber mixtures: part i. neoprene-carbon black mixtures. *Polymer degradation and stability*, 35(1):49–52, 1992.
- [65] Daegue Park, Agrim Gupta, Shayaun Bashar, Cédric Girerd, Dinesh Bharadia, and Tania K Morimoto. Design and evaluation of a miniaturized force sensor based on wave backscattering. *IEEE Robotics and Automation Letters*, 7(3):7550–7557, 2022.
- [66] Living Systems Instrumentation. Tungsten wire (20 um diameter / 1m length). *Living Systems Instrumentation*, 2022.
- [67] Henry K Chu, James K Mills, and William L Cleghorn. Design of a high sensitivity capacitive force sensor. In *2007 7th IEEE Conference on Nanotechnology (IEEE NANO)*, pages 29–33. IEEE, 2007.
- [68] Yu Sun and Bradley J Nelson. Mem capacitive force sensors for cellular and flight biomechanics. *Biomedical Materials*, 2(1):S16, 2007.
- [69] NXP. SL3ics1002/1202. [https://www.nxp.com/docs/en/data-sheet/SL3ICS1002\\_1202.pdf](https://www.nxp.com/docs/en/data-sheet/SL3ICS1002_1202.pdf), 2022.
- [70] Inhee Lee, Roger Hsiao, Gordy Carichner, Chin-Wei Hsu, Mingyu Yang, Sara Shoouri, Katherine Ernst, Tess Carichner, Yuyang Li, Jaechan Lim, et al. msail: milligram-scale multi-modal sensor platform for monarch butterfly migration tracking. In *Proceedings of the 27th Annual International Conference on Mobile Computing and Networking*, pages 517–530, 2021.
- [71] Github Repo. Sllurp. <https://github.com/sllurp/sllurp>, 2022.
- [72] Github Repo. Sllurp-gui. <https://github.com/fviard/sllurp-gui>, 2022.
- [73] Raunaq Bhirangi, Tess Hellebrekers, Carmel Majidi, and Abhinav Gupta. Reskin: versatile, replaceable, lasting tactile skins. *arXiv preprint arXiv:2111.00071*, 2021.
- [74] Deepak Vasisht, Guo Zhang, Omid Abari, Hsiao-Ming Lu, Jacob Flanz, and Dina Katabi. In-body backscatter communication and localization. In *Proceedings of the 2018 Conference of the ACM Special Interest Group on Data Communication*, pages 132–146, 2018.
- [75] Sandeep KS Gupta, Suresh Lalwani, Yashwanth Prakash, E Elsharawy, and Loren Schwiebert. Towards a propagation model for wireless biomedical applications. In *IEEE International Conference on Communications, 2003. ICC'03.*, volume 3, pages 1993–1997. IEEE, 2003.
- [76] Ilka Dove. Analysis of radio propagation inside the human body for in-body localization purposes. Master’s thesis, University of Twente, 2014.
- [77] Farzan Dehbashi, Ali Abedi, Tim Brecht, and Omid Abari. Verification: can wifi backscatter replace rfid? In *Proceedings of the 27th Annual International Conference on Mobile Computing and Networking*, pages 97–107, 2021.
- [78] Xiaoran Fan, Longfei Shangguan, Richard Howard, Yanyong Zhang, Yao Peng, Jie Xiong, Yunfei Ma, and Xiang-Yang Li. Towards flexible wireless charging for medical implants using distributed antenna system. In *Proceedings of the 26th annual international conference on mobile computing and networking*, pages 1–15, 2020.
- [79] Zihan Zhao, Xihui Mu, and Fengpo Du. Modeling and verification of a new hyperelastic model for rubber-like materials. *Mathematical Problems in Engineering*, 2019, 2019.
- [80] Xiuzhen Guo, Longfei Shangguan, Yuan He, Nan Jing, Jiacheng Zhang, Haotian Jiang, and Yunhao Liu. Saiyan: Design and implementation of a low-power demodulator for {LoRa} backscatter systems. In *19th USENIX Symposium on Networked Systems Design and Implementation (NSDI 22)*, pages 437–451, 2022.
- [81] Vamsi Talla, Mehrdad Hesar, Bryce Kellogg, Ali Najafi, Joshua R Smith, and Shyamnath Gollakota. Lora backscatter: Enabling the vision of ubiquitous connectivity. *Proceedings of the ACM on interactive, mobile, wearable and ubiquitous technologies*, 1(3):1–24, 2017.
- [82] Pat Pannuto, Benjamin Kempke, and Prabal Dutta. Slocalization: Sub-uw ultra wideband backscatter localization. In *2018 17th ACM/IEEE International Conference on Information Processing in Sensor Networks (IPSN)*, pages 242–253. IEEE, 2018.
- [83] Michael Fonseca, Mark Allen, David Stern, Jason White, and Jason Kroh. Implantable wireless sensor for pressure measurement within the heart, February 15 2005. US Patent 6,855,115.
- [84] David Hana Issa Pour-Ghaz, Joel Raja, Uzoma N Ibebuogu, and Rami N Khouzam. Cardiomems: where we are and where can we go? *Annals of translational medicine*, 7(17), 2019.
- [85] Dongjin Seo, Ryan M Neely, Konlin Shen, Utkarsh Singhal, Elad Alon, Jan M Rabaey, Jose M Carmena, and Michel M Maharbiz. Wireless recording in the peripheral nervous system with ultrasonic neural dust. *Neuron*, 91(3):529–539, 2016.
- [86] Cheng Chi, Xuguang Sun, Ning Xue, Tong Li, and Chang Liu. Recent progress in technologies for tactile sensors. *Sensors*, 18(4):948, 2018.
- [87] Ravinder S Dahiya, Philipp Mitterdorfer, Maurizio Valle, Gordon Cheng, and Vladimir J Lumelsky. Directions toward effective utilization of tactile skin: A review. *IEEE Sensors Journal*, 13(11):4121–4138, 2013.

- [88] Mahesh Soni and Ravinder Dahiya. Soft eskin: distributed touch sensing with harmonized energy and computing. *Philosophical Transactions of the Royal Society A*, 378(2164):20190156, 2020.
- [89] Liang Zou, Chang Ge, Z Jane Wang, Edmond Cretu, and Xiaoou Li. Novel tactile sensor technology and smart tactile sensing systems: A review. *Sensors*, 17(11):2653, 2017.
- [90] Patrick Parzer, Kathrin Probst, Teo Babic, Christian Rendl, Anita Vogl, Alex Olwal, and Michael Haller. Flexiles: a flexible, stretchable, formable, pressure-sensitive, tactile input sensor. In *Proceedings of the 2016 CHI Conference Extended Abstracts on Human Factors in Computing Systems*, pages 3754–3757, 2016.
- [91] Patrick Parzer, Florian Perteneder, Kathrin Probst, Christian Rendl, Joanne Leong, Sarah Schuetz, Anita Vogl, Reinhard Schwoediauer, Martin Kaltenbrunner, Siegfried Bauer, et al. Resi: a highly flexible, pressure-sensitive, imperceptible textile interface based on resistive yarns. In *Proceedings of the 31st Annual ACM Symposium on User Interface Software and Technology*, pages 745–756, 2018.
- [92] Andreas Pointner, Thomas Preindl, Sara Mlakar, Roland Aigner, and Michael Haller. Knitted resi: A highly flexible, force-sensitive knitted textile based on resistive yarns. In *ACM SIGGRAPH 2020 Emerging Technologies*, pages 1–2, 2020.
- [93] Hyosang Lee, Kyungseo Park, Yunjoo Kim, and Jung Kim. Durable and repairable soft tactile skin for physical human robot interaction. In *Proceedings of the Companion of the 2017 ACM/IEEE International Conference on Human-Robot Interaction*, pages 183–184, 2017.
- [94] Bruno Gil, Bing Li, Anzhu Gao, and Guang-Zhong Yang. Miniaturized piezo force sensor for a medical catheter and implantable device. *ACS applied electronic materials*, 2(8):2669–2677, 2020.
- [95] Haoyan Zang, Xianmin Zhang, Benliang Zhu, and Sergej Fatikow. Recent advances in non-contact force sensors used for micro/nano manipulation. *Sensors and Actuators A: Physical*, 296:155–177, 2019.
- [96] Tess Hellebrekers, Nadine Chang, Keene Chin, Michael J Ford, Oliver Kroemer, and Carmel Majidi. Soft magnetic tactile skin for continuous force and location estimation using neural networks. *IEEE Robotics and Automation Letters*, 5(3):3892–3898, 2020.
- [97] Harshal A Sonar, Michelle C Yuen, Rebecca Kramer-Bottiglio, and Jamie Paik. An any-resolution pressure localization scheme using a soft capacitive sensor skin. In *2018 IEEE International Conference on Soft Robotics (RoboSoft)*, pages 170–175. IEEE, 2018.
- [98] Divya Ramesh, Qiyuan Fu, and Chen Li. Sensnake: A snake robot with contact force sensing for studying locomotion in complex 3-d terrain. *arXiv preprint arXiv:2112.09078*, 2021.
- [99] Ann Marie Votta, Sezen Yağmur Günay, Deniz Erdoğan, and Çağdaş Önal. Force-sensitive prosthetic hand with 3-axis magnetic force sensors. In *2019 IEEE International Conference on Cyborg and Bionic Systems (CBS)*, pages 104–109. IEEE, 2019.
- [100] Anany Dwivedi, Anand Ramakrishnan, Aniketh Reddy, Kunal Patel, Selim Ozel, and Cagdas D Onal. Design, modeling, and validation of a soft magnetic 3-d force sensor. *IEEE Sensors Journal*, 18(9):3852–3863, 2018.
- [101] Chen Li, Qiulin Tan, Pinggang Jia, Wendong Zhang, Jun Liu, Chenyang Xue, and Jijun Xiong. Review of research status and development trends of wireless passive lc resonant sensors for harsh environments. *Sensors*, 15(6):13097–13109, 2015.
- [102] Qing-An Huang, Lei Dong, and Li-Feng Wang. Lc passive wireless sensors toward a wireless sensing platform: status, prospects, and challenges. *Journal of Microelectromechanical Systems*, 25(5):822–841, 2016.
- [103] Clementine M Boutry, Levent Beker, Yukitoshi Kaizawa, Christopher Vassos, Helen Tran, Allison C Hinckley, Raphael Pfattner, Simiao Niu, Junheng Li, Jean Claverie, et al. Biodegradable and flexible arterial-pulse sensor for the wireless monitoring of blood flow. *Nature biomedical engineering*, 3(1):47–57, 2019.
- [104] Junbo Zhang, Gaurav Balakrishnan, Sruti Srinidhi, Arnav Bhat, Swarun Kumar, and Christopher Bettinger. Nfcapsule: An ingestible sensor pill for eosinophilic esophagitis detection based on near-field coupling. In *Proceedings of the Twentieth ACM Conference on Embedded Networked Sensor Systems*, pages 75–90, 2022.
- [105] Marco Baù, Marco Demori, Marco Ferrari, and Vittorio Ferrari. Contactless readout of passive lc sensors with compensation circuit for distance-independent measurements. In *Multidisciplinary Digital Publishing Institute Proceedings*, volume 2, page 842, 2018.
- [106] Haining Li, Jiexiong Ding, Siqi Wei, Bowen Chu, Lichao Guan, Li Du, Guangmin Liu, and Jianguo He. A miniature layered saw contact stress sensor for operation in cramped metallic slits. *Instruments and Experimental Techniques*, 61(4):610–617, 2018.
- [107] Xiaohua Yi, Terence Wu, Yang Wang, Roberto T Leon, Manos M Tentzeris, and Gabriel Lantz. Passive wireless smart-skin sensor using rfid-based folded patch antennas. *International Journal of Smart and Nano Materials*, 2(1):22–38, 2011.
- [108] Trang T Thai, Herve Aubert, Patrick Pons, Manos M Tentzeris, and Robert Plana. Design of a highly sensitive wireless passive rf strain transducer. In *2011 IEEE MTT-S International Microwave Symposium*, pages 1–4. IEEE, 2011.
- [109] JR Humphries and DC Malocha. Passive, wireless saw ofc strain sensor. In *2012 IEEE International Frequency Control Symposium Proceedings*, pages 1–6. IEEE, 2012.
- [110] Lijun Teng, Kewen Pan, Markus P Nemitz, Rui Song, Zhirun Hu, and Adam A Stokes. Soft radio-frequency identification sensors: Wireless long-range strain sensors using radio-frequency identification. *Soft robotics*, 6(1):82–94, 2019.
- [111] Cédric Girerd, Qiming Zhang, Agrim Gupta, Manideep Dunna, Dinesh Bharadia, and Tania K Morimoto. Towards a wireless force sensor based on wave backscattering for medical applications. *IEEE Sensors Journal*, 21(7):8903–8915, 2021.
- [112] Xingyu Chen, Jia Liu, Fu Xiao, Shigang Chen, and Lijun Chen. Thermotag: item-level temperature sensing with a passive rfid tag. In *Proceedings of the 19th Annual International Conference on Mobile Systems, Applications, and Services*, pages 163–174, 2021.

- [113] Azhar Hasan, Rahul Bhattacharyya, and Sanjay Sarma. Towards pervasive soil moisture sensing using rfid tag antenna-based sensors. In *2015 IEEE International Conference on RFID Technology and Applications (RFID-TA)*, pages 165–170. IEEE, 2015.
- [114] Ju Wang, Liqiong Chang, Shourya Aggarwal, Omid Abari, and Srinivasan Keshav. Soil moisture sensing with commodity rfid systems. In *Proceedings of the 18th International Conference on Mobile Systems, Applications, and Services*, pages 273–285, 2020.
- [115] Emran Md Amin, Rahul Bhattacharyya, Sanjay Sarma, and Nemaï C Karmakar. Chipless rfid tag for light sensing. In *2014 IEEE Antennas and Propagation Society International Symposium (APSURSI)*, pages 1308–1309. IEEE, 2014.
- [116] Meng-Ju Hsieh, Jr-Ling Guo, Chin-Yuan Lu, Han-Wei Hsieh, Rong-Hao Liang, and Bing-Yu Chen. Rftouchpads: Batteryless and wireless modular touch sensor pads based on rfid. In *Proceedings of the 32nd Annual ACM Symposium on User Interface Software and Technology*, pages 999–1011, 2019.
- [117] Swadhin Pradhan, Eugene Chai, Karthikeyan Sundaresan, Lili Qiu, Mohammad A Khojastepour, and Sampath Rangarajan. Rio: A pervasive rfid-based touch gesture interface. In *Proceedings of the 23rd Annual International Conference on Mobile Computing and Networking*, pages 261–274, 2017.
- [118] Nicolai Marquardt, Alex S Taylor, Nicolas Villar, and Saul Greenberg. Rethinking rfid: awareness and control for interaction with rfid systems. In *Proceedings of the SIGCHI Conference on Human Factors in Computing Systems*, pages 2307–2316, 2010.
- [119] Alanson P Sample, Daniel J Yeager, and Joshua R Smith. A capacitive touch interface for passive rfid tags. In *2009 IEEE International Conference on RFID*, pages 103–109. IEEE, 2009.
- [120] Timothy M Simon, Bruce H Thomas, Ross T Smith, and Mark Smith. Adding input controls and sensors to rfid tags to support dynamic tangible user interfaces. In *Proceedings of the 8th International Conference on Tangible, Embedded and Embodied Interaction*, pages 165–172, 2014.
- [121] Albrecht Schmidt, H-W Gellersen, and Christian Merz. Enabling implicit human computer interaction: a wearable rfid-tag reader. In *Digest of Papers. Fourth International Symposium on Wearable Computers*, pages 193–194. IEEE, 2000.
- [122] Chuhan Gao, Yilong Li, and Xinyu Zhang. Livetag: Sensing human-object interaction through passive chipless wifi tags. In *15th {USENIX} Symposium on Networked Systems Design and Implementation ({NSDI} 18)*, pages 533–546, 2018.
- [123] Hanchuan Li, Can Ye, and Alanson P Sample. Idsense: A human object interaction detection system based on passive uhf rfid. In *Proceedings of the 33rd Annual ACM Conference on Human Factors in Computing Systems*, pages 2555–2564, 2015.